

國立交通大學

電機學院光電顯示科技產業研發碩士班
碩士論文

人眼視覺導向之低功耗液晶顯示器背光管理

**Visual Perception-Guided Low-Power LCD
Backlight Management**



研究生：趙健富
指導教授：鄭惟中 博士

中華民國九十六年二月

人眼視覺導向之低功耗液晶顯示器背光管理

Visual Perception-Guided Low-Power LCD Backlight Management

研究生: 趙健富

Student: Chien-Fu Chao

指導教授: 鄭惟中 博士

Advisor: Dr. Wei-Chung Cheng

國立交通大學

電機學院光電顯示科技產業研發碩士班

碩士論文

A Thesis

Submitted to College of Electrical and Computer Engineering

National Chiao Tung University

in Partial Fulfillment of the Requirements

for the Degree of

Master

in

Industrial Technology R & D Master Program on

Photonics and Display Technologies

February 2007

Hsinchu, Taiwan, Republic of China

中華民國九十六年二月

人眼視覺導向之低功耗液晶顯示器背光管理

碩士研究生：趙健富

指導教授：鄭惟中 博士

國立交通大學 電機學院

中文摘要

以人眼視覺感受為導向，我們提供了一個三色背光調節(backlight scaling)的演算法，藉著影像的統計圖，分別調節該影像紅、藍、綠三色的背光強度。該演算法分成二部分，第一部分為色度調節，在一個給定的色差條件下找出紅、藍、綠三色光的比率。第二部分為亮度調節，在可察覺的明度差異下調節背光模組的亮度，同時，我們利用心理物理實驗去找到最佳的亮度轉移函數。為了實現該演算法，我們並架設一組實驗平台來量測實行演算法之後的效果。在所有選定的測試影像(benchmark image)中，我們量測出最多可以節省55%的LED背光模組功率消耗，且兼顧該顯示影像的品質。

Visual Perception-Guided Low-Power LCD Backlight Management

Student : Chien-Fu Chao

Advisor : Dr. Wei-Chung Cheng

National Chiao Tung University

ABSTRACT

This study presents an algorithm for minimizing power consumption of LED backlights in transmissive TFT-LCD monitors. The proposed algorithm reduces power consumption by scaling the luminous intensity of the red, green, and blue LED backlights independently according to the image histograms of each color channel. The algorithm consists of two phases. The first phase, chromaticity scaling, finds the optimal ratios of red, green, and blue backlights subject to a perceived color difference constraint. The second phase, luminance scaling, finds the optimal dimming factor subject to a perceived lightness difference constraint. The perceived color and lightness differences are measured by the CIELAB Color Difference Equation $2 \Delta E_{ab}^*$, a standard metric for measuring color variation. Psychophysical experiments were performed to uncover the optimal luminance scaling function. The Chromaticity-Luminance Scaling algorithm was implemented in a prototype. Within limited perceivable difference $2 \Delta E_{ab}^*$, up to 55% of power consumption can be reduced for the benchmark images.

致 謝

回憶這兩年的日子，有歡欣的微笑也有辛勤的汗水。一路上，受到眾人的扶持與關懷，讓我能夠順利完美地劃下句點。在此，謹以該論文表達對你們誠摯的謝意。

兩年的研究生活與論文的完成，首先要感謝鄭惟中老師，您不只提供優良的學習環境，也給予我學習機會，並且花費不少精神和時間指導我，不僅讓我在專業工具、語言、做事方法各方面都具有相當顯著的提升，更重要的是讓我有更具彈性的思維以及正向的思考，並用不同層面的觀點來看待事物及問題，在此誠心的謝謝您！

在這段求學的日子裡，感謝所有研究所的好夥伴枝福、淑萍、建智、俊文、俞文、映頻、愷均、浩瑜、佳峰、明倫等，在課業上、研究上、生活上的幫助與分享，因為有你們，我的研究生活變得十分有趣，另可能尚有未提及但是曾經幫助過我的朋友們，在此均一併致謝。你們的陪伴讓我在兩年的研究生活過的快樂又充實。在此，特別要感謝枝福和淑萍，不論是我在研究過程或是生活方面遇到挫折或困難，你們都不吝於給我幫助和建議，充分予我堅持到底的力量，讓我順利完成我的學位，謝謝你們！

最後感謝我的家人們，是你們在我背後默默的支持，讓我毫無後顧之憂，專注在自己的學習崗位上。因為你們的付出與鼓勵，堅定我辭去工作重拾書本的信念，最後我可以順利完成我的研究，沒有你們的付出和支持，我相信今天的我不會有如此的成就，在這裡表達我最由衷的感謝，也將這篇論文獻給我最摯愛的家人們。

Table of Contents

摘要	iii
Abstract	iv
致謝	v
Table of Contents	vi
List of Tables	viii
List of Figures	ix
Chapter 1 Introduction	1
1.1 TFT-LCDs architecture	2
1.2 Backlight Scaling	4
1.3 Spatial Color Synthesis and Temporal Color Synthesis	5
1.4 Motivation and Objective	7
1.5 Organization	7
Chapter 2 Previous Works of Backlight Management	9
2.1 Summary	9
Chapter 3 Principle: Assess Visual Quality	12
3.1 Photometric Definitions	12
3.2 Colorimetry	13
3.3 Color Appearance Terminology	16
3.4 Psychophysics	17
3.4.1 Method of Adjustment	18
3.4.2 Method of Limits	18
3.5 Stevens Effect	18
3.6 Bartleson-Breneman Effect	20
Chapter 4 Psychophysical Experiments	22
4.1 Objective and Background	22
4.2 Perceived Brightness versus Contrast in Sinusoidal Grating Pattern	22
4.3 Perceived Brightness versus Perceived Contrast in Complex Stimuli	25
4.3.1 Darkroom and Apparatus	25
4.3.2 Procedure	27
4.3.3 Experimental Results	28

4.4 Summary.....	29
Chapter 5 Proposed Algorithm.....	31
5.1 Chromaticity Scaling.....	31
5.2 Luminance Scaling.....	33
5.3 Summary.....	34
Chapter 6 Prototype.....	35
6.1 Framework.....	35
6.1.1 Image Processing Flow.....	36
6.2 Block Diagram of Prototype.....	37
6.2.1 Low Voltage Differential Signaling.....	38
6.3 Platform.....	40
6.3.1 Experimental Panel.....	40
6.3.2 FPGA Board.....	41
6.3.3 LED backlight.....	42
6.3.4 Instruments and Equipment.....	43
6.3.5 Platform Block Diagram.....	44
6.4 FPGA Architecture.....	45
6.4.1 Display Signal.....	45
6.4.2 LVDS Interface / TFT Data (Color) Mapping.....	48
6.4.3 Implementation of Algorithm.....	49
6.4.4 Hardware Cost.....	55
6.5 Summary.....	55
Chapter 7 Measuremental Results.....	57
7.1 Hardware characterization.....	57
7.1.1 Panel.....	57
7.1.2 LED backlights.....	58
7.2 Results and discussion.....	59
7.2.1 Power Savings.....	60
7.2.2 Performance.....	62
7.2.3 Viewing Angle Enhancement for Visual Effect.....	63
7.3 Summary.....	65
Chapter 8 Conclusion and Future Direction.....	66
8.1 Conclusion.....	66
8.2 Future Direction.....	67
References.....	68

List of Tables

Table 6-1. The FPGA chip usage.....	55
Table 7-1. Benchmark images.	61
Table 7-2. Optimal solutions for benchmark images subject to $\Delta E_{ab}^* \leq 1$ and $\Delta E_{ab}^* \leq 2$	62



List of Figures

Figure 1-1. TFT-LCD Architecture.	3
Figure 1-2. LCD subsystem architecture.....	3
Figure 1-3. PC system and LCD component architecture.....	4
Figure 1-4. Power, backlight, transmittance, and luminance.	4
Figure 1-5. Spatial color synthesis and temporal color synthesis.....	6
Figure 1-6. The red, green, and blue field of a frame.....	6
Figure 2-1. <i>Night Watch</i> (a) Rembrandt (b) Choi (c) Iranli (d) Cheng.....	9
Figure 3-1. Illustration of LED backlight and photometric terms.....	12
Figure 3-2. The CIE color matching functions for the 1931 Standard Colorimetric Observer.....	14
Figure 3-3. The CIE x,y chromaticity diagram.	15
Figure 3-4. CIE-Lab chromaticity diagram.	16
Figure 3-5. Results of determining the brightness functions under different states of adaptation [24].....	19
Figure 3-6. Change in lightness contrast as function of adapting luminance according to the Stevens effect [25].	20
Figure 3-7. Changes in lightness contrast as a function of surround relative luminance according to the results of Bartleson and Breneman [22][29].....	20
Figure 4-1. The experimental apparatus.....	23
Figure 4-2. The sinusoidal grating pattern with varied apparent brightness and contrast.	23
Figure 4-3. Contrast versus related luminance.	25
Figure 4-4. The setup of darkroom.....	26
Figure 4-5. The LED lights.....	26
Figure 4-6. TFT-LCD monitors used in the experiments.	27
Figure 4-7. GretagMacBeth Eye-One XT.....	27
Figure 4-8. Matching the original softcopy (left) with the contrast-adjusted one (right).....	28
Figure 4-9. The image contrast was modulated between high (left) and low (right).	28
Figure 4-10. Subject count vs. contrast adjustment for ascending (bottom) and descending (top) trials.	29
Figure 4-11. Contrast fidelity vs. contrast.	30
Figure 5-1. Photo and R, G, and B histogram.....	31
Figure 5-2. Procedure of finding backlight factor.	33

Figure 5-3. Transfer functions of chromaticity and luminance scaling.....	34
Figure 6-1. Backlight scaling of portable electronic device.....	35
Figure 6-2. Our notion of backlight scaling.	36
Figure 6-3. Block diagram of image processing flow.	37
Figure 6-4. Fetching the image data as the image data is delivered by graphic card.	38
Figure 6-5. Fetching the image data as the image data passes the scaler board.....	38
Figure 6-6. Simplified diagram of LVDS driver and receiver.	39
Figure 6-7. VX912 monitor and panel.....	40
Figure 6-8. Block diagram of the AUO panel.	41
Figure 6-9. Xilinx Spartan-3 Starter Kit Board [31].	42
Figure 6-10. LED and LED backlight.	43
Figure 6-11. Block diagram of backlight module.....	43
Figure 6-12. LED backlight driving board.	43
Figure 6-13. Chroma meter.....	44
Figure 6-14. Power supply.....	44
Figure 6-15. Multimeter.....	44
Figure 6-16. Layout of experimental system.....	45
Figure 6-17. Waveform chart of video signal (a).	47
Figure 6-18. Waveform chart of video signal (b).	47
Figure 6-19. Waveform chart of video signal (c).	48
Figure 6-20. TTL data inputs mapped to LVDS outputs [32].....	49
Figure 6-21. Basic hierarchy of the HDL code.....	50
Figure 6-22. The histogram calculation module.....	50
Figure 6-23. The boundary determination block.	51
Figure 6-24. The circuit scheme of backlight adjusting hierarchy.	52
Figure 6-25. The PWM Generator.	52
Figure 6-26. The circuit scheme of transmittance adjusting hierarchy.....	53
Figure 6-27. The block diagram of the FPGA chip.	54
Figure 6-28. Experimental setup.	56
Figure 7-1. Pixel transmittance versus power consumption of a pixel in the normally white TFT-LCD panel.	58
Figure 7-2. Power consumption vs. PWM duty cycle.....	58
Figure 7-3. Luminance vs. PWM duty cycle.....	59
Figure 7-4. Photos of prototype LED backlit (left) and CCFL-lit (right) system, where $b_R=0.9$, $b_G=0.8$, and $b_B=0.7$. From top to bottom: $b_L=1.0$, 0.8, and 0.6.....	60
Figure 7-5. Comparison between the original images and the scaling images.	63
Figure 7-6. Color shift of the panel of VX912 at different viewing angles.....	64
Figure 7-7. The panels were tilted about 30° vertical viewing angle.....	65

Chapter 1

Introduction

Power consumption has become the critical issue for battery powered electronics. In literature, researchers have found that the display consumes a major portion of the total power consumption in portable devices. These devices, which are developed to trend toward smaller and lighter, are usually powered by small-sized rechargeable batteries. Unfortunately, the rechargeable battery capacities are increasing at a much slower pace than the overall power dissipation of these devices. Therefore, it is critical to develop low-power design technique for reducing the power consumption of these electronic devices.

However, battery lifetime becomes the most important feature for mobile electronics. Recently, Liquid Crystal Displays (LCDs) have appeared in applications ranging from medical equipment to mobile electronics such as cell phones, personal digital assistants, digital still cameras, camcorders, laptop computers, etc. The LCD displays currently available require two power sources, a backlight supply and a panel supply. Previous studies point out that the display subsystem dominates the energy consumption of a mobile system [1]. Moreover, in a transmissive display, the backlight contributes most of the power consumption. The dominant backlighting technology for the conventional LCDs is the Cold Cathode Fluorescent Lamp (CCFL), which uses a DC-to-AC converter as the driver. The driver consumes the largest amount of power in the display system. In addition, the CCFL backlight has disadvantages, includes larger size, low response time, with mercury, etc. Due to these issues, more advanced backlight devices have emerged to replace the CCFL such as light-emitting diode (LED).

In the past, LCD power consumption has been treated primarily from a hardware optimization viewpoint. Several hardware optimization techniques focus on the mixed-signal

circuits that drive the pixel matrix [2][3][4], or on the methods for storing charge in the matrix capacitors [5], which are beyond the scope of our work.

To prolong battery lifetime, a low-power design technology has been developed for minimizing the power consumed by the backlight. The concept of *Backlight Scaling* was proposed by the researchers [6][7][8]. The approach of backlight scaling technology is lowering the power consumption of the LCD backlight system. Furthermore, the image quality is conserved.

1.1 TFT-LCDs architecture

The main components of a transmissive TFT-LCD display subsystem include the video controller, frame buffer, video interface, TFT-LCD panel, and backlight. The frame buffer is a portion of memory used by software applications to deliver video data to the video controller. The video data, which is received from the processing unit, is first saved into the frame buffer memory by the video controller and is subsequently transmitted to the LCD controller through an appropriate analog (VGA) or digital (Digital Video Interface -- DVI) interface.

The video interface carries the video signals between the video controller and the TFT-LCD display. The TFT-LCD display receives the video data and generates proper transmittance for each pixel according to its pixel value. All of the pixels on the transmissive LCD panel are illuminated by the backlight from behind. To the observer, if the transmittance of a displayed pixel is high, the pixel looks bright. On the other hand, a displayed pixel looks dark if its transmittance is low. If the transmittance can be adjusted to more than two different levels, then the pixels can be displayed in grayscale. If the shade can be colored as red, green, or blue by using different color filters, then pixels can be displayed in color by mixing three sub-pixels in different colors at different grayscales. In other words, the perceived brightness of a pixel is determined by its transmittance and the backlight luminous intensity. A

normally-white TFT-LCDs architecture is shown in Figure 1-1.

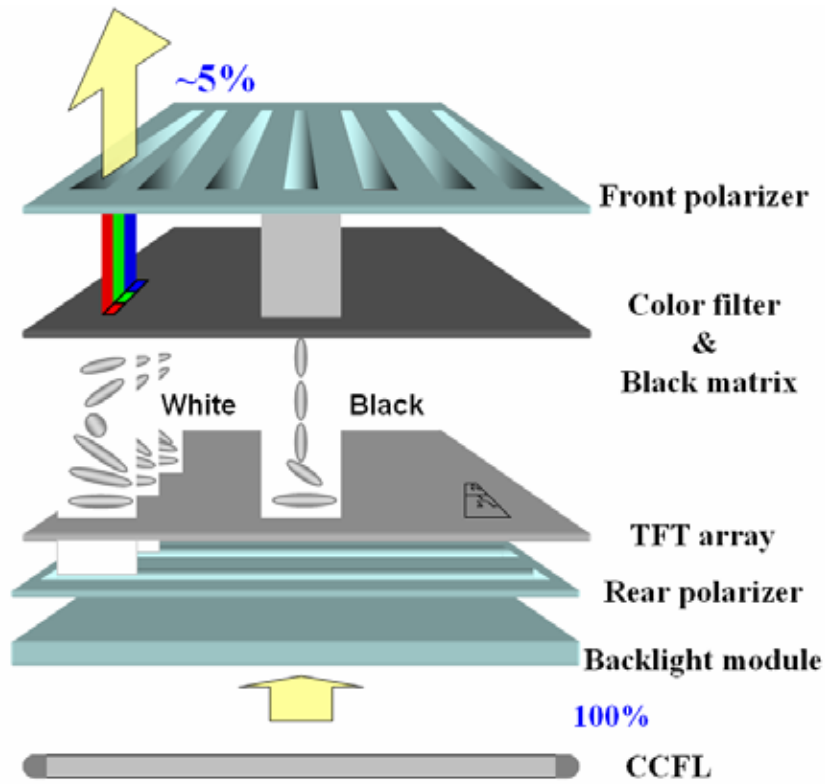


Figure 1-1. TFT-LCD Architecture.

Figure 1-2 shows the typical architecture of the digital LCD subsystem including the video controller/frame buffer memory and LCD controller/panel.

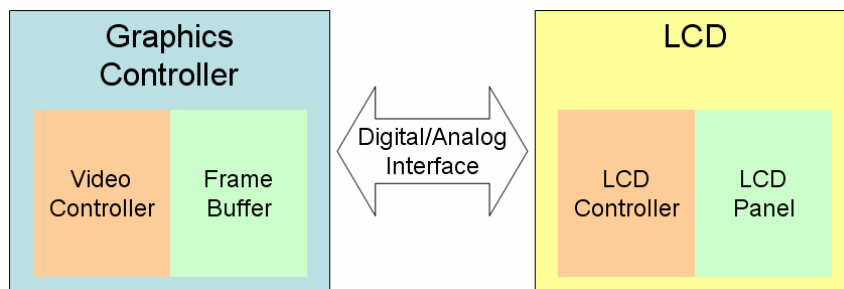


Figure 1-2. LCD subsystem architecture.

Figure 1-3 shows the LCD components. The data received from the video bus is used to infer timing information and respective grayscale levels. Then, this timing information is used to select the appropriate row in the LCD matrix. Next, the pixel values are converted to the corresponding voltage levels to drive the thin-film-transistors (TFT) on different columns of

the selected row. The backlight is powered with the aid of a DC-AC converter, to provide the required illumination.

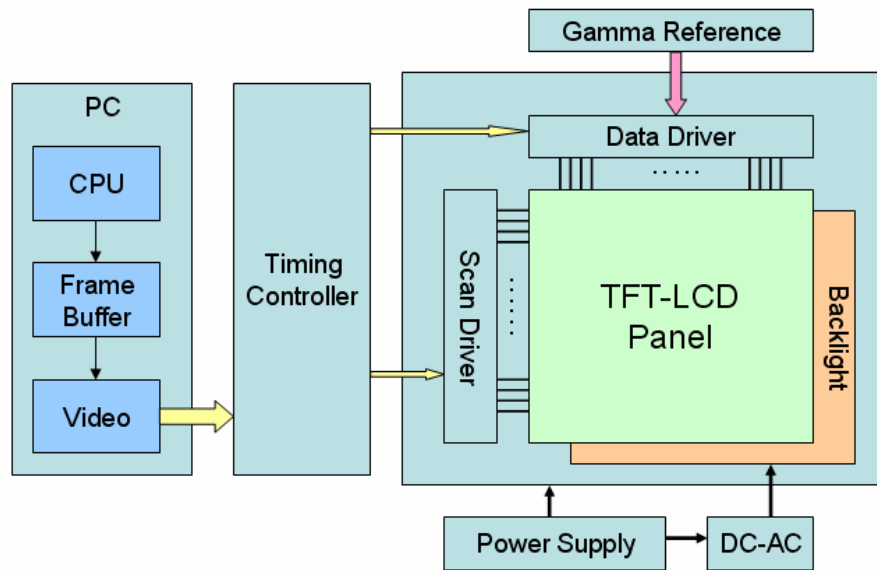


Figure 1-3. PC system and LCD component architecture.

1.2 Backlight Scaling



The concept of *backlight scaling* is simply dimming the backlight to conserve power consumption and to increase image quality.

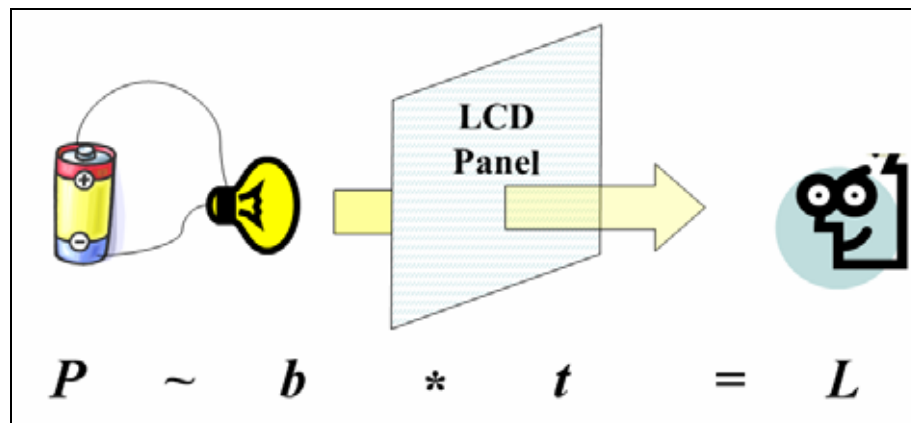


Figure 1-4. Power, backlight, transmittance, and luminance.

The luminance of LCD perceived by the user is the product of the backlight luminous intensity (b) and the panel transmittance (t):

$$L = b \cdot t \quad (1-1)$$

The power consumption of the backlight is a strong function of its output luminance. On the contrary, the power consumption of the LCD panel is almost constant so that it is independent of the panel transmittance. Therefore, we can decrease the backlight luminous intensity b to save the power consumption P . The panel transmittance t is increased accordingly such that the luminance L remains the same. In addition, higher transmittance can reduce the light leakage phenomenon of liquid crystals and increase the image quality.

Consider a pixel consisting of red, green, and blue sub-pixel. Its color is determined by the product of the backlight luminous intensity and the transmittance of each sub-pixel:

$$\begin{bmatrix} L_R \\ L_G \\ L_B \end{bmatrix} = b_W \cdot \begin{bmatrix} t_R \\ t_G \\ t_B \end{bmatrix} \quad (1-2)$$

$L_R:L_G:L_B$ is the luminance ratio of red, green, and blue. For example, white is obtained at the ratio of 3:6:1. An LCD generates different colors by changing the transmittance ratio of sub-pixels $t_R:t_G:t_B$.

If the backlight module uses red, green, and blue backlight instead of a single white backlight, then the pixel color can be represented by

$$\begin{bmatrix} L_R \\ L_G \\ L_B \end{bmatrix} = \begin{bmatrix} b_R & 0 & 0 \\ 0 & b_G & 0 \\ 0 & 0 & b_B \end{bmatrix} \begin{bmatrix} t_R \\ t_G \\ t_B \end{bmatrix} \quad (1-3)$$

In this case, the pixel color depends on not only the transmittance ratio but also the ratio of RGB backlights $b_R:b_G:b_B$. This equation can be applied to both spatial and temporal methods of synthesizing colors.

1.3 Spatial Color Synthesis and Temporal Color Synthesis

Most displays use either spatial or temporal method to synthesize colors (Figure 1-5). The CRT and TFT-LCD monitors use the spatial method. On the 2-dimensional screen, a color pixel consists of three sub-pixels: red, green and blue. The temporal method is used by projector displays, which produce the red, green, and blue components sequentially in a very short time period such that human vision cannot perceive the separation. This method is called *field sequential display* or *color sequential display*.

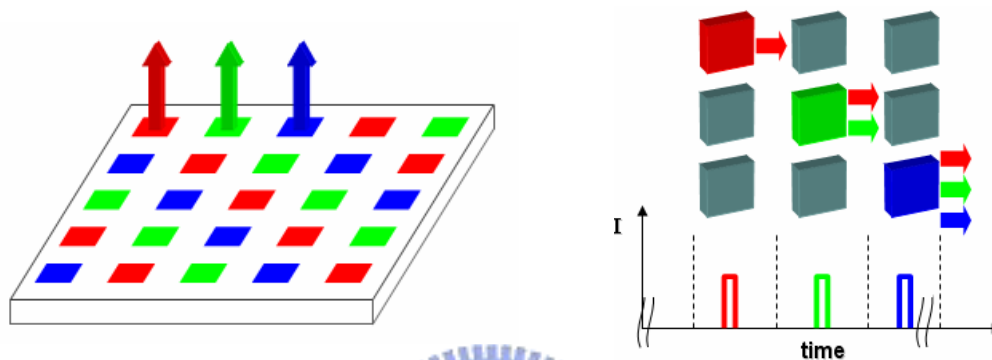


Figure 1-5. Spatial color synthesis and temporal color synthesis.

In the color sequential display, a frame is decomposed into red, green, and blue fields, which are displayed sequentially. The three fields are illuminated by the red, green, and blue backlight accordingly, while the luminance of each color is controlled by panel transmittance.



Figure 1-6. The red, green, and blue field of a frame.

Unlike the spatial method, where a pixel consists of three sub-pixels, in a color sequential display, the RGB components of a pixel share the same estate on panel. Therefore, the pixel

density of a color sequential display can be increased to three times, which translates into 3 times display resolution (i.e., smaller pixel pitch for finer images) or 1/3 display size (for miniature displays such as head-mounted displays). The color sequential technology has been widely used in projection displays based on either the digital light processor (DLP) or LCD technology.

1.4 Motivation and Objective

The backlight dominates the power consumption of an LCD system. Our goal is to reduce the power consumption of the LCD backlight. The battery lifetime of mobile electronic devices can be prolonged. The technique, backlight scaling is used to reduce the power consumption of LCD backlight.

This scaling requires an algorithm to process. Using Brute-force algorithm in backlight scaling is a conventional method to save power consumption, but it reduces brightness, and thus, the display quality is degraded. Our objective is to dim the backlight intensity without sacrificing the visual quality. To achieve the maximum power savings for a given color distortion limit, we propose algorithms of backlight scaling for minimizing power consumption of LED backlights.

1.5 Organization

This thesis is organized as follows. The previous works and the features of backlight scaling will be presented in Chapter 2. In Chapter 3, the principles including photometric definitions, colorimetry, color appearance terminology and psychophysics will be discussed. In Chapter 4, two psychophysical experiments and experimental results will be described. The proposed algorithm of backlight scaling will be introduced in Chapter 5. In Chapter 6, the fabrication of experimental platform and measurement equipments will be illustrated. The

experimental results will be shown in Chapter 7. Finally, the conclusion of the thesis and the future work are given in Chapter 8.



Chapter 2

Previous Works of Backlight Management

In this chapter the previous works of backlight management are summarized.

2.1 Summary

Backlight scaling is by far the most effective technique for reducing power consumption in a transmissive display. This technique scales down the backlight luminous intensity to save power consumption at the cost of reduced image luminance, which results in lower visual quality. To compensate for the visual quality loss due to reduced luminance, proper image enhancement is necessary.



Figure 2-1. *Night Watch* (a) Rembrandt (b) Choi (c) Iranli (d) Cheng.

As mentioned before (2.1-2.3), different image enhancement algorithms for backlight

scaling have been proposed in the past years. Choi *et al.* proposed a technique that increases the pixel values (t) to recover the original luminance (L) [7]. However, the transmittance t in Equation 1-1 is bounded by 0 and 1. When t needs to be greater than 1, the original luminance can not be recovered and image distortion occurs. Choi's algorithm can preserve the luminance of the dark regions, but the bright regions will be over-saturated. In their work, the number of over-saturated pixels was chosen to evaluate the image quality loss. Apparently the approach of preserving luminance L is too conservative, so preserving alternative objectives, such as a transformation on the luminance, $L^* = f(L)$, have been proposed by the other groups [13]. In addition, a series of studies were proposed in [14][15][16][17]. All of their algorithm used the same image-enhancement method for preserving luminance and restrict to image quality loss by the different conditions. They implemented their algorithm by a server and network.

Iranli *et al.* proposed using *histogram equalization*, an image processing algorithm that balances the number of pixels on each graylevel, to perform the image enhancement [12]. The transformation is the cumulative distribution function of the histogram. Histogram equalization can reproduce each graylevel distinctly without over-saturation or under-saturation. However, the proportional difference between bright and dark regions, i.e., *tonality*, will be distorted greatly when the original histogram tends to be irregular. Figure 2-1 shows such an example.

While the other researchers treat the backlight scaling problem in the brightness domain (pixel values), the same authors proposed another work that emphasizes on the mapping between luminance and brightness, commonly referred as *gamma correction* [18]. Gamma correction is one of the standard features for modern displays such that the end users can adjust their monitors for different viewing condition, user preferences, manufacturing variations, and luminance/color degradation as aging.

Cheng *et al.* proposed an algorithm to compensate for the luminance loss by increasing

the contrast [10]. The following linear transformation was used:

$$\begin{bmatrix} L_R^* \\ L_G^* \\ L_B^* \end{bmatrix} = c \begin{bmatrix} L_R - gl \\ L_G - gl \\ L_B - gl \end{bmatrix} \quad (2-1)$$

Although Cheng's algorithm is a compromise between preserving the brightness and preserving the contrast, it does preserve the original tonality. The relationship between brightness and contrast, however, was employed without substantial support.

The visual effects of different image enhancement algorithms are shown in Figure 2-1. The original image with 100% backlighting is shown in Figure 2-1a, in which most pixels are either very bright or very dark. Figure 2-1 show Choi's, Iranli's, and Cheng's results with backlight scaled to 50%.

The minimal perceivable radiant flux from a display was calculated from the aspect of human factors by Zhong *et al.* in [19]. The authors concluded that the comfortable reading luminance is seven orders of magnitude larger than the just-perceptible threshold. However, such pure radiometric calculation is oversimplified without considering the other dominating human vision factors such as light adaptation and dark adaptation [20]. For example, for the classical just-noticeable difference (JND) data to be valid, the ambient light cannot be ignored, since the adaptation mechanism of human eyes can change visual sensitivity by five orders of magnitude.

In a nutshell, the principle of backlight scaling is to trade perceived image quality for power savings. In our work, we employ the results and methods that were well established in vision study, color science, psychophysical experiments to design our proposed backlight scaling algorithm.

Chapter 3

Principle: Assess Visual Quality

The research of backlight scaling involves photometry, colorimetry, psychophysics, etc. The key concepts and terminologies are reviewed in this section.

3.1 Photometric Definitions

Though light is a form of electromagnetic radiation, measurement of luminous intensity from a light source requires extra information about the relative sensitivity of the human eye to different wavelengths. Photometry is the science of measurement of the intensity of visible light and its illuminating power according to the sensitivity of the human eye. The following photometric quantities are illustrated around a TFT-LCD display in Figure 3-1.

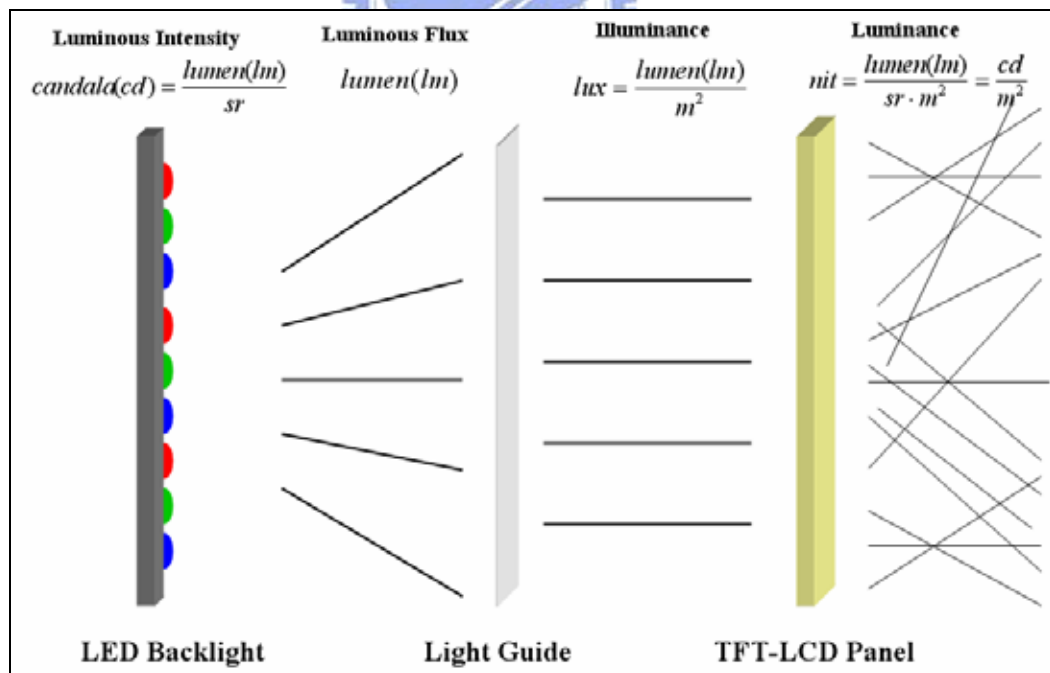


Figure 3-1. Illustration of LED backlight and photometric terms.

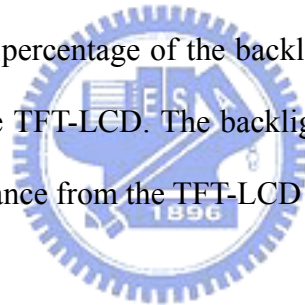
Luminous flux (lumen): is the emission rate of light energy corrected for the standardized spectral response of human vision.

Luminous intensity (candela): is defined as $\text{cd}=\text{lm}/\text{sr}$, one lumen of luminous flux per steradian (unit of solid angle). Luminous intensity can be used to characterize the optical power emitted from a spot light source, such as a light bulb.

Illuminance (lux): is defined as one lumen of luminous flux per area (lm/m^2). Illuminance can be used to characterize the luminous power emitted from a surface. Most light meters (e.g., for photographic purpose) measure the illuminance quantity. The luminous flux may not travel in parallel after passing the surface, so that the light intensity decreases as the travel distance increases.

Luminance (nit) is physical measure, and defined as lumen per area per steradian ($\text{lm} / \text{m}^2 / \text{sr}$ or cd / m^2) [10][20].

Luminance is used to rate the maximum brightness of CRT or LCD monitors. We use backlight factor to express the percentage of the backlight illumination, and transmissivity to express the transparency of the TFT-LCD. The backlight factor and TFT-LCD transmissivity determine the perceived luminance from the TFT-LCD display.



3.2 Colorimetry

The human eyes have three types of *cones* perceiving light at different wavelengths. The *L*-, *M*-, and *S*-cones respond to, roughly, the wavelengths of red, green, and blue – the *primaries*. Mixing the three primaries in different ratios generates different *colors*. The colors can be ordered in different ways and be represented by different *color spaces*. Computers use the *RGB* color space, which is convenient for the graphics adaptor and displays. Printers use the *CMY* color space or its variation. In color science, a color space usually consists of the one-dimensional *luminance* and the two-dimensional *chromaticity*. For a color, luminance indicates its magnitude, while chromaticity indicates the ratio between red, green and blue. *Colorimetry* is the discipline of determining and specifying colors of objects by standardizing

the observer, illuminator, viewing geometry, etc. Most *de facto* color spaces were defined by CIE, the International Commission on Illumination. The CIE standard observer was defined by standardizing the *color matching functions*, the response function of red (x), green (y), and blue (z) as shown in Figure 3-2.

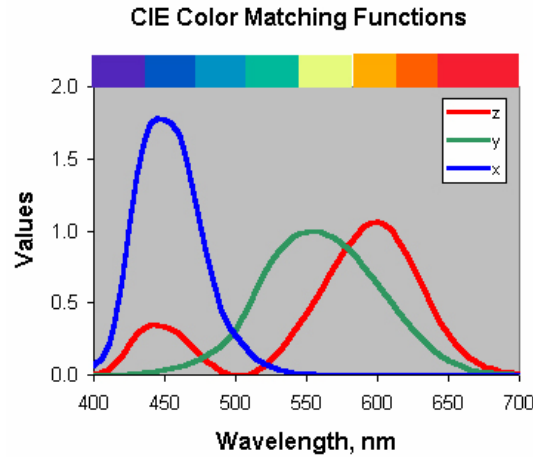


Figure 3-2. The CIE color matching functions for the 1931 Standard Colorimetric Observer.

Once the standard observer is defined, the *CIE XYZ* color space can be obtained by defining the X , Y , and Z values (in uppercase) as the product of spectral power distribution of the object Φ and the color matching function (x, y, z) across wavelength λ :

$$\begin{aligned}
 X &= k \int_{\lambda} \Phi(\lambda) \bar{x}(\lambda) d\lambda, \\
 Y &= k \int_{\lambda} \Phi(\lambda) \bar{y}(\lambda) d\lambda, \\
 Z &= k \int_{\lambda} \Phi(\lambda) \bar{z}(\lambda) d\lambda.
 \end{aligned}
 \tag{3-1}$$

To separate the luminance component from chromaticity, the x , y , z values are defined as

$$\begin{aligned}
 x &= \frac{X}{X + Y + Z}, \\
 y &= \frac{Y}{X + Y + Z}, \\
 z &= \frac{Z}{X + Y + Z}.
 \end{aligned}
 \tag{3-2}$$

Since there are only two dimensions of information in chromaticity coordinates, the third

chromaticity coordinate can always be obtained from the other two by noting that the three always sum to unity. Thus z can be calculated from x and y using Equation (3-3).

$$z = 1.0 - x - y \quad (3-3)$$

The x , y , and z value represent chromaticity, the ratio between red, green, and blue, which is independent of luminance. The z value is redundant because it can be obtained from x and y . The two-dimensional chromaticity diagram of CIEXYZ is shown in Figure 3-3. The horseshoe shape depicts the range of visible colors. The Euclidean distance between two different colors can be used to measure their color difference. However, CIEXYZ is not an ideal color space because the color difference is not perceived uniformly. For example, for the same color difference, a pair of blue colors is perceived more differently than a pair of green colors.

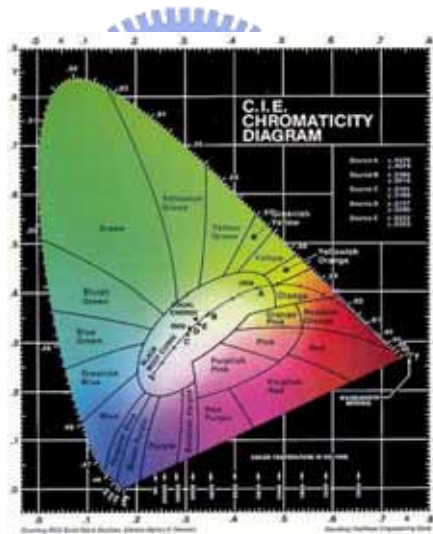


Figure 3-3. The CIE x,y chromaticity diagram.

A more uniform color space, CIELAB, is defined by

$$L^* = 116\left(\frac{Y}{Y_n}\right)^{1/3} - 16,$$

$$a^* = 500\left[\left(\frac{X}{X_n}\right)^{1/3} - \left(\frac{Y}{Y_n}\right)^{1/3}\right], \quad (3-4)$$

$$b^* = 200\left[\left(\frac{Y}{Y_n}\right)^{1/3} - \left(\frac{Z}{Z_n}\right)^{1/3}\right].$$

The CIELAB ΔE_{ab}^* color difference is defined by

$$\Delta E_{ab}^* = \sqrt{(\Delta L^*)^2 + (\Delta a^*)^2 + (\Delta b^*)^2}. \quad (3-5)$$

The ΔE_{ab}^* color difference is considered as a uniform metric and has been widely used and implemented in commercial colorimeters.

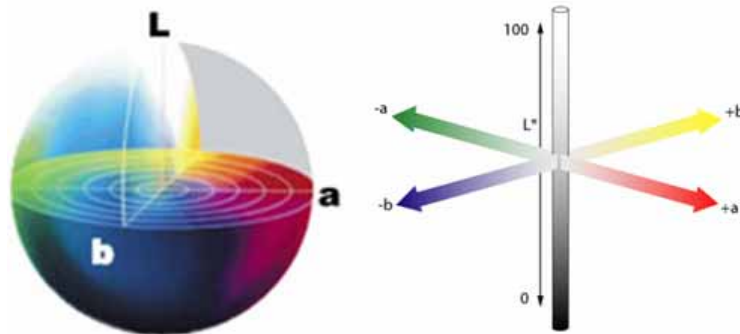


Figure 3-4. CIE-Lab chromaticity diagram.

3.3 Color Appearance Terminology

The following definitions introduced in this chapter have been culled from the International Lighting Vocabulary [20].

Brightness: attribute of a visual sensation according to which an area appears to emit more or less light.

Lightness: the brightness of an area judged relative to the brightness of a similarly illuminated area that appears to be white or highly transmitting.

Besides, another very important concept is contrast. The following definitions are adopted from Fairchild [22]. There are two different definitions for contrast. One definition for contrast, which is used in tone reproduction, is the rate of change of the relative luminance of image elements of a reproduction as a function of the relative luminance of the same image elements of the original image. On log-log coordinates, the contrast is the slope of the relationship between the reproduction and original. The contrast defined in this way is an

attribute of the system transfer function.

Another definition for contrast, which is used in visual science, is the difference between minimum and maximum luminance in an image. This contrast is an attribute of the image. The perceived image contrast is the perceived lightness difference between dark part and the light part of an image.

3.4 Psychophysics

Psychophysics is the scientific study of the relationships between the physical measurements of stimuli and the sensations and perceptions that those stimuli evoke. Psychophysics can be considered a discipline of science similar to the more traditional disciplines such as physics, chemistry, and biology.

The tools of psychophysics are used to derive quantitative measures of perceptual phenomena that are often considered subjective. It is important to note that the results of properly designed psychophysical experiments are just as objective and quantitative as the measurement of length with a ruler or any other physical measurement. One important difference is that the uncertainties associated with psychophysical measurements tend to be significantly larger than those of physical measurements. However, the results are equally useful and meaningful as long as those uncertainties are considered as they always should be for physical measurements as well. Psychophysics is used to study all dimensions of human perception.

In our work, two threshold techniques proposed by Fechner were used [22][23]. The threshold experiments were designed to determine the just-perceptible change in a stimulus, sometimes referred to as a just-noticeable difference, which is used to measure the observers' sensitivity to changes in a given stimulus. Absolute thresholds are defined as the just-perceptible difference for a change from no stimulus, while difference thresholds

represent the just-perceptible difference from a particular stimulus level greater than zero.

3.4.1 Method of Adjustment

The method of adjustment is the simplest and most straightforward technique for deriving threshold data. In this method, the observer controls the stimulus magnitude and adjusts it to a point that is just visible. The threshold is taken to be the average setting across a number of trials by one or more observers.

3.4.2 Method of Limits

The method of limits is only slightly more complex than the method of adjustment. With this method, the experimenter presents the stimuli at predefined discrete intensity levels in either ascending or descending series. In the ascending series, the experimenter presents a stimulus, beginning with one that is certain to be imperceptible, and asks the observers to respond 'yes' if they perceive it and 'no' if they do not. If they respond 'no', the experimenter increases the stimulus intensity. The descending series begins with a stimulus intensity that is clearly perceptible and continues until the observers respond 'no', they cannot perceive the stimulus. The threshold is taken to be the average stimulus intensity at which the transition from 'no' to 'yes' responses occurs for a number of ascending and descending series.

3.5 Stevens Effect

According to the classic psychophysical brightness scaling experiment from Stevens, perceived brightness could be expressed as power function of physical luminance [24].

$$\psi = k(L - L_0)^\beta \quad (3-6)$$

where k is a constant, β is brightness (psychological magnitude), L is luminance, L_0 is the absolute threshold value. All the parameters, k , L_0 , and β change systematically with light

adaptation. The exponent β increases from 0.33 for the dark-adapted eye to 0.44 for the eye adapted to 1 lambert.

Furthermore, in J. C. Stevens and S. S. Stevens' study, observers were asked to perform magnitude estimations on the brightness of stimuli across various adapting conditions. The results illustrated that the relationship between perceived brightness and measured luminance tended to follow a power function.

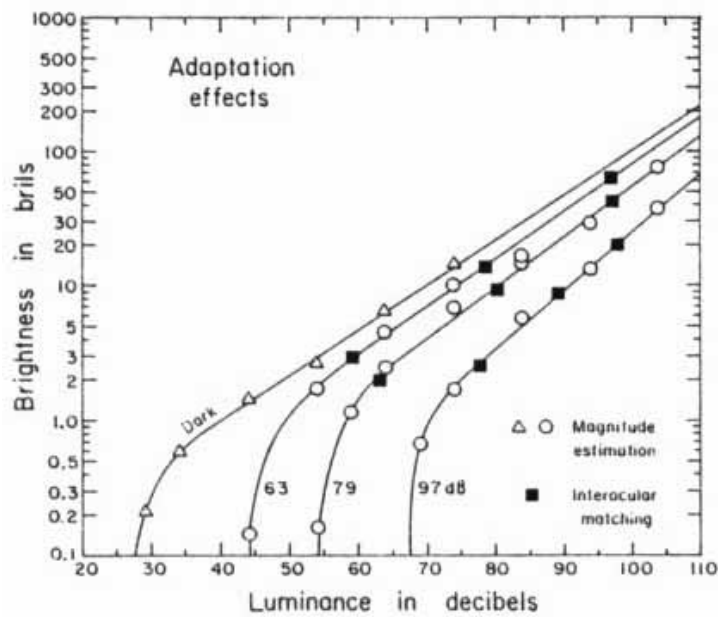


Figure 3-5. Results of determining the brightness functions under different states of adaptation [24].

A relationship that follows a power function when plotted on linear coordinates becomes a straight line on log-log coordinates, and shows in Figure 3-6. The Stevens effect indicates that, as the luminance level increases, dark colors will appear darker and light colors will appear lighter. While Stevens effect was demonstrated by viewing an image at high and low luminance levels, a black-and-white image is particularly effective for this demonstration. At a low luminance level, the image will appear of rather low contrast. White areas will not appear very bright, and the dark areas will not appear very dark. If the image is then moved to a significantly higher level of illumination, white areas appear substantially brighter and dark areas darker, it meant the perceived contrast has increased.

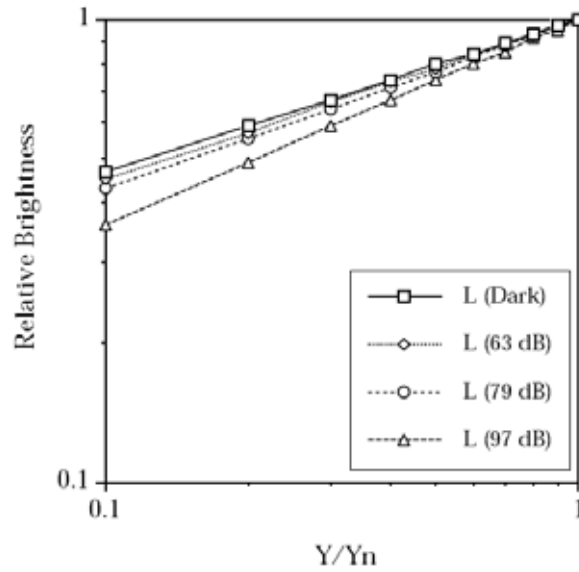


Figure 3-6. Change in lightness contrast as function of adapting luminance according to the Stevens effect [25].

3.6 Bartleson-Breneman Effect

Bartleson and Breneman conducted psychophysical experiments to investigate the perceived contrast of elements in complex stimuli (images) and how it varied with luminance level and surround [26]. Their experimental results were similar to those described by the Stevens effect with respect to luminance changes. They also observed some interesting results with respect to changes in the relative luminance of an image's surround.

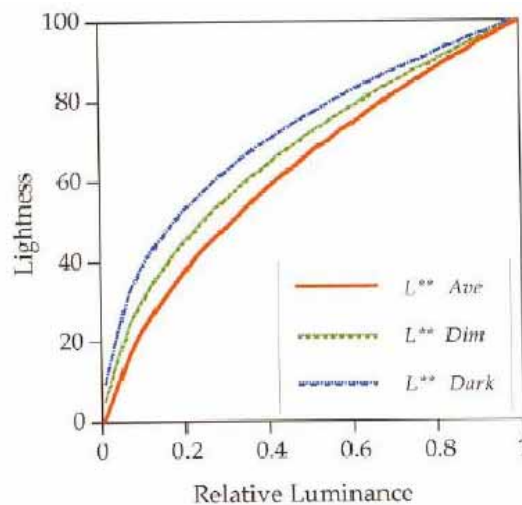


Figure 3-7. Changes in lightness contrast as a function of surround relative luminance according to the results of Bartleson and Breneman [22][29].

Their experimental results, obtained through matching and scaling experiments, showed that the perceived contrast of images increased when the image surround was changed from dark to dim to light. This effect occurs because the dark surround of an image causes areas to appear lighter while having little effect on light areas. Thus, since there is more of a perceived change in the dark areas of an image than in the light areas, there is a resultant change in perceived contrast.



Chapter 4

Psychophysical Experiments

4.1 Objective and Background

In Chapter 3, two well-known visual phenomena are introduced. They both are associated with contrast. The Stevens' effect predicts that the perceived contrast of a simple stimulus (e.g. color) increases with the surround illumination [24]. The Bartleson-Breneman effect predicts that the perceived contrast of complex stimuli (e.g. an image) increases with the surround illumination [26]. Recently, the relationship between image contrast and surround illumination was studied by Liu [27]. However, the interaction between brightness and apparent contrast of complex stimuli has not been investigated yet.

The goal of this study is to establish the relation between perceived brightness and apparent contrast of natural images, and apply the results to display designs such as power minimization of transmissive TFT-LCDs. Our objective is to answer the following question: When the brightness of an image is reduced, can we compensate for it by increasing its contrast? If the answer is positive, then this concept can be used in low-power applications.

In this study, psychophysical experiments were employed to find the answer of the question. The psychophysical experiment consists of two steps. In the first step, the sinusoidal grating pattern was equipped for validating the interaction between perceived contrast and brightness. Furthermore, the complex stimuli were used to explore the same approach.

4.2 Perceived Brightness versus Contrast in Sinusoidal Grating Pattern

The psychophysical experiments were conducted in a dedicated darkroom. The experimental setup and apparatus are shown in Figure 4-1. A 17" CRT monitor (Viewsonic

E71f) was used to display the sinusoidal grating patterns, which were generated by MATLAB. The resolution of the CRT is 1024×768, and the sinusoidal grating pattern in center of the display is 256×256. The distance between the observer and the monitor is 150cm.

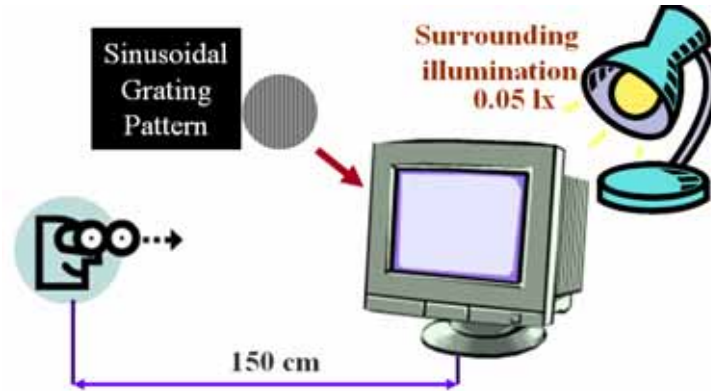


Figure 4-1. The experimental apparatus.

The sinusoidal grating pattern, which had 1.6 circles per degree (CPD), was vertically divided into two parts as left-hand side and right-hand side. The pattern of left-hand side presented the original pattern, which had reduced brightness; the right-hand side one presented the contrast-enhanced pattern. However, the patterns of both sides can be switched randomly for the purpose of psychophysical experiments, which are shown in Figure 4-2.

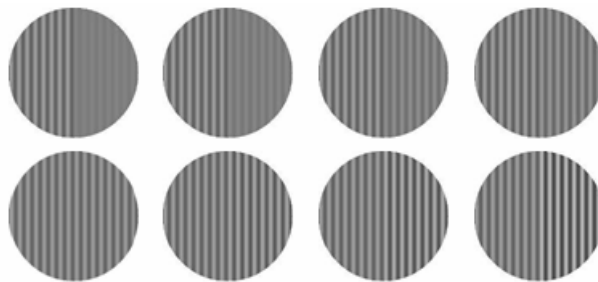


Figure 4-2. The sinusoidal grating pattern with varied apparent brightness and contrast.

We used *method of adjustment*, a classical psychophysical method [23]. The original pattern was reduced brightness from 100% to 60%. The experiment was divided into eight trials. Each trial consists of a series of differently contrast-enhanced patterns according to reduced brightness of the original pattern. If the variation of contrast enhanced patterns was too high, these patterns will not be compared with the original pattern. The margin of

contrast-enhanced pattern was limited to 200%. Each observer was asked to compare the original pattern against a series of differently contrast-enhanced patterns, and to find the most resemble one. In order to avoid the observer guessing the resemble pattern, the patterns of right-hand side and left-hand side were switched randomly. It meant the original pattern and contrast-enhanced pattern were not fixed on the same side.

Four observers were enlisted as subjects in the experiments. They were Asian male, aged from 23 to 29, and have normal vision after lens correction. Before starting the experiments, the subjects were asked to adapt the surround illumination for 30 seconds. Figure 4-3 shows the experimental results of four subjects as contrast vs. related brightness in the eight trials. Each curve represents an individual observer. All curves show the same tendency. This tendency points out the subjects agreed on the same isoluminance point under increasing contrast while the brightness was reduced. However, we were specifically interested in the region of brightness between 0.7 and 0.9. The experimental results show the relation between the contrast-enhancement and related brightness is close to linear in this region. The results indicate the subjects had similar perception while they viewed the two sinusoidal patterns -- one without adjustment and the other with reduced brightness and enhanced contrast -- in a specific region. Thus, the interaction between the apparent contrast and brightness is validated.

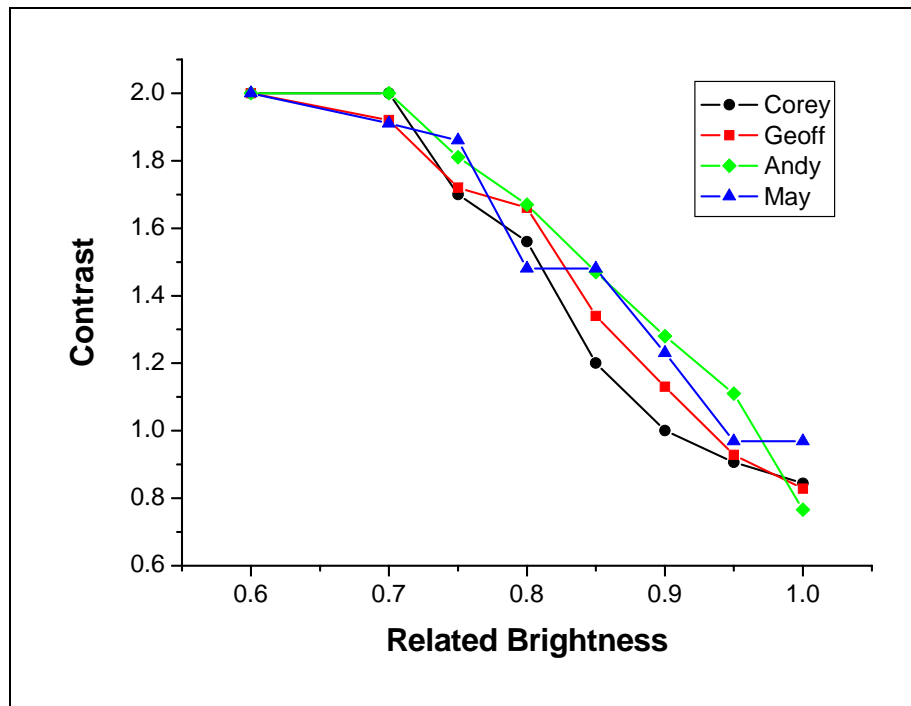


Figure 4-3. Contrast versus related luminance.

4.3 Perceived Brightness versus Perceived Contrast in Complex Stimuli

In this study, we investigated the relationship between perceived image brightness and contrast by conducting psychophysical experiments. Thirty-seven observers were enlisted to perform visual experiments of determining the optimal contrast enhancement with reduced brightness.

4.3.1 Darkroom and Apparatus

The experiments were conducted in a light-proof darkroom, in which the measurable illumination is less than 0.03 lx (cf. Figure 4-4).

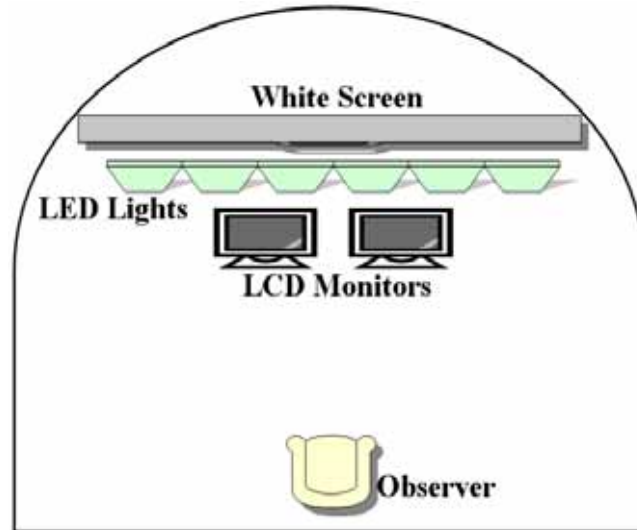


Figure 4-4. The setup of darkroom.

A set of six identical LED lights were installed for controlling the surround illumination. Each LED light contains three channels -- red, green, and blue. The luminance and chromaticity of the six LED lights can be controlled freely (cf. Figure 4-5). The surround illumination was projected on a white screen as the field of view. A pair of identical transmissive 19" TFT-LCD monitors (Viewsonic VX912) was used to display the test images (cf. Figure 4-6). They were driven by the same computer, and color-corrected by a GretagMacBeth Eye-One XT spectrophotometer (cf. Figure 4-7).



(a) LED light.



(b) The LED lights project white surround.

Figure 4-5. The LED lights.



Figure 4-6. TFT-LCD monitors used in the experiments.



Figure 4-7. GretagMacBeth Eye-One XT.

4.3.2 Procedure

The psychophysical experiments were performed for three different levels of surround – 0%, 50%, and 100% of the full luminance of the monitors. The test image was chosen from a popular set of benchmark images from the HDR research community (www.devevec.org). The original softcopy was displayed by the left-hand-side monitor with 100% of backlighting. The contrast-adjusted softcopy was displayed by the right-hand-side monitor with 70% of backlighting. The adjusted image was displayed on the right with 70% of backlight intensity after the following contrast enhancement

$$p_L = MAX \{0, MIN \{1, (p_L - \bar{m})slope + \bar{m}\}, 0\}, \quad \bar{m} = 126 / 255 \quad (4-1)$$

Most of the thirty-seven observers were Asian male, aged from 22 to 28, and have normal vision after lens correction. The subjects were screened by a simple Ishihara Color

Deficiency Test, and two of them were excluded based on the test results.

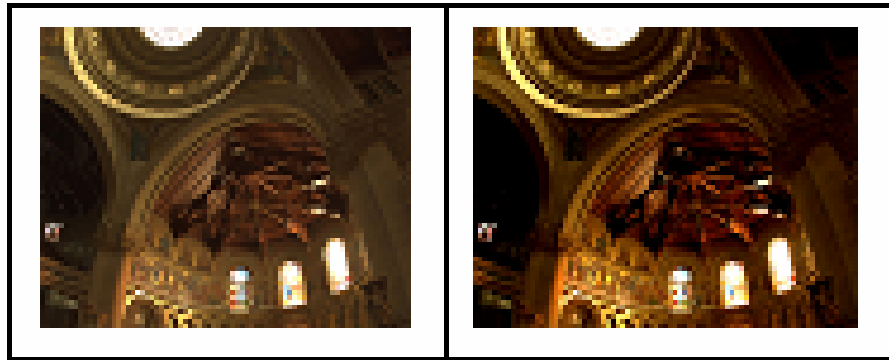


Figure 4-8. Matching the original softcopy (left) with the contrast-adjusted one (right).

The experiment started with a 30 seconds period for the subject to adapt to the surround illumination while the monitors displayed gray fields of the same luminance. The subject was asked to match the original softcopy with the contrast-adjusted one (cf. Figure 4-8). The classical psychophysical method, *Method of Limits* [23], was used. A series of differently contrast-enhanced images in ascending/descending order was displayed sequentially (cf. Figure 4-9).

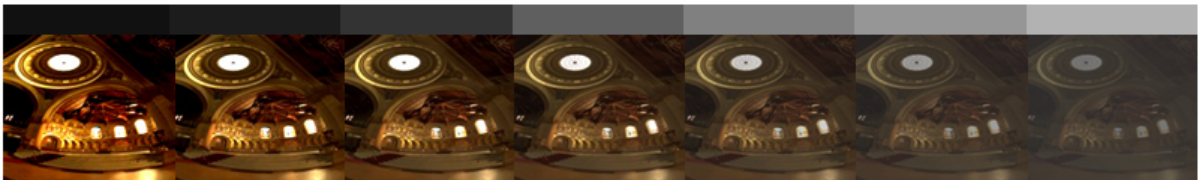


Figure 4-9. The image contrast was modulated between high (left) and low (right).

The subject had to decide if the point of isoluminance was reached. The corresponding contrast adjustment at the point of isoluminance was recorded for analysis. The experiments were repeated for three times with surround at 0%, 50%, and 100%.

4.3.3 Experimental Results

Figure 4-10 shows the experimental data as subject count vs. contrast adjustment in the ascending and descending trials. The top/bottom curve represents the descending/ascending

data. Each point indicates the number of subjects who agreed on the same isoluminance point.

Both ascending and descending distributions are near Gaussian with a mean value around 120% contrast-adjustment. It indicates that most subjects agreed on this point of isoluminance. The mean of the ascending trial is greater than that of the descending trial. The reason is the persistence of visual perception, which is common in experiments using Method of Limits.

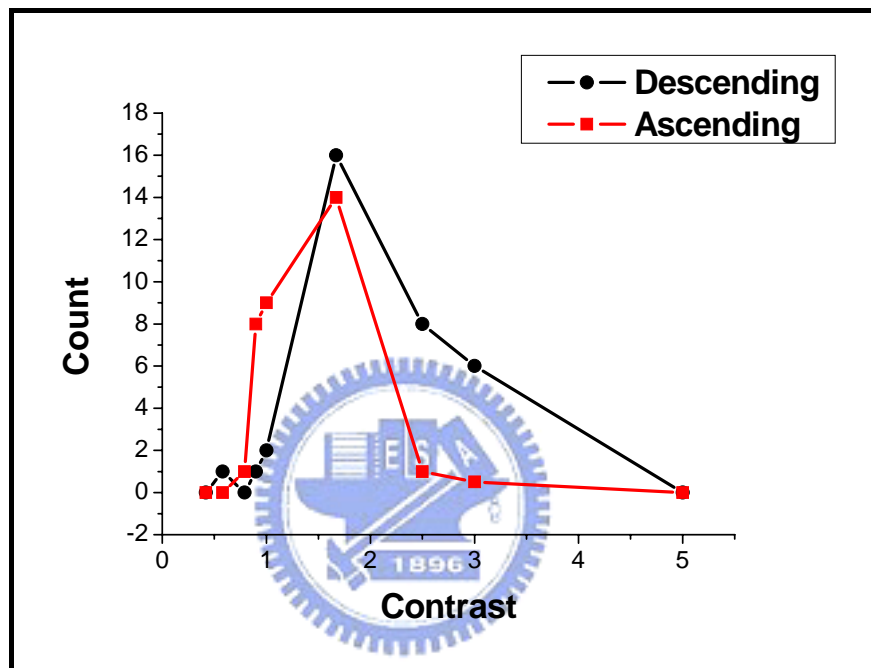


Figure 4-10. Subject count vs. contrast adjustment for ascending (bottom) and descending (top) trials.

4.4 Summary

According to the experimental results, decreased brightness can be compensated by increasing luminance contrast. The experimental results can be applied to low-power display design. In a transmissive TFT-LCD, reducing the backlight intensity to save power consumption, at the cost of degraded image quality, is a common practice. Based on our findings, one can increase the contrast to recover the image quality.

To compare our psychophysical results with [10], we calculated the image quality of the

same image. The relation between image quality and contrast enhancement is shown in Figure 4-11.

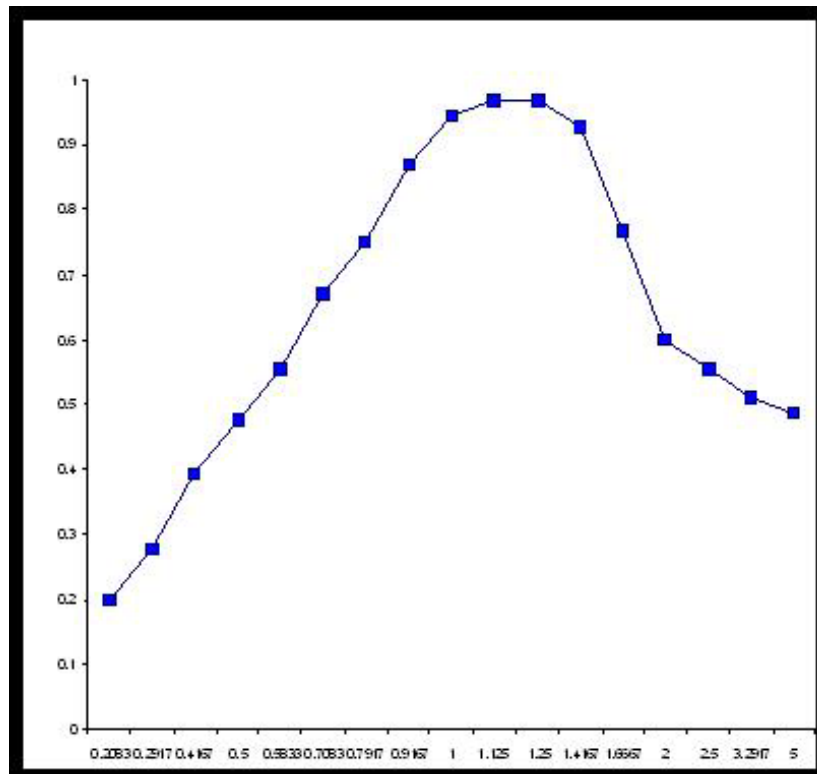


Figure 4-11. Contrast fidelity vs. contrast.

We found high resemblance between Figure 4-10 and Figure 4-11. In other words, for the given image, our psychophysical findings are in accordance with the analytical model in [10]. Although further experiments are undergoing for more concrete conclusions, in this work we adopted the CBCS algorithm.

Chapter 5

Proposed Algorithm

We propose a backlight scaling algorithm for an LED backlit display. The proposed algorithm consists of two phases. In the first phase, *chromaticity scaling*, the image is chromatically scaled subject to the perceivable colorfulness difference. The optimal ratio of RGB backlights is found to achieve maximum power savings at the same luminance. In the second phase, *luminance scaling*, the luminance is scaled down to achieve maximum power savings subject to the perceivable lightness difference.

5.1 Chromaticity Scaling



Figure 5-1. Photo and R, G, and B histogram.

The motivation of chromaticity scaling is that most images have different distributions in their RGB histograms. To achieve more power savings, the RGB channels can be scaled differently. For example, in Figure 5-1, in average the red channel has higher luminance than the blue channel does. This observation implies that the blue backlight can be scaled down more than the red backlight. However, the side effect of scaling RGB channels differently is color shift. Therefore, we use the color difference defined by Equation (3-5) to govern the chromaticity scaling. We define the following notation to represent an image after

chromaticity scaling.

$$I(b_R, b_G, b_B) \equiv p_{i \in \{R, G, B\}} = \begin{cases} p_i, & p_i \leq b_i \\ b_i, & p_i > b_i \end{cases} \quad (5-1)$$

When the red, green, and blue backlight are down-scaled from 1.0 to b_R , b_G , and b_B respectively, the red, green, and blue sub-pixel will be clipped by b_R , b_G , and b_B respectively.

We use $\Delta E(I_1, I_2)$ to indicate the average color difference between the original image I_1 and chromaticity-scaled image I_2 . Given Q as the color shift constraint, the following algorithm finds the optimal chromaticity scaling factors that save the most power consumption with the least color shift. The procedure of finding backlight factor shows in Figure 5-2.

Chromaticity_Scaling:

$$S_R = \Delta E_{ab}^*(I(1,1,1), I(b_R - \delta, b_G, b_B)) / P_R(b_R - \delta);$$

$$S_G = \Delta E_{ab}^*(I(1,1,1), I(b_R, b_G - \delta, b_B)) / P_G(b_G - \delta);$$

$$S_B = \Delta E_{ab}^*(I(1,1,1), I(b_R, b_G, b_B - \delta)) / P_B(b_B - \delta);$$

Find $MIN(S_R, S_G, S_B)$, whose $\Delta E_{ab}^* \leq Q$;

if (found) then

Depend on $MIN(S_R, S_G, S_B)$, *update either* b_R , b_G , *or* b_B *with* $b_R - \delta$, $b_G - \delta$, *or* $b_B - \delta$

accordingly;

goto Chromaticity_Scaling;

else

return b_R , b_G , and b_B

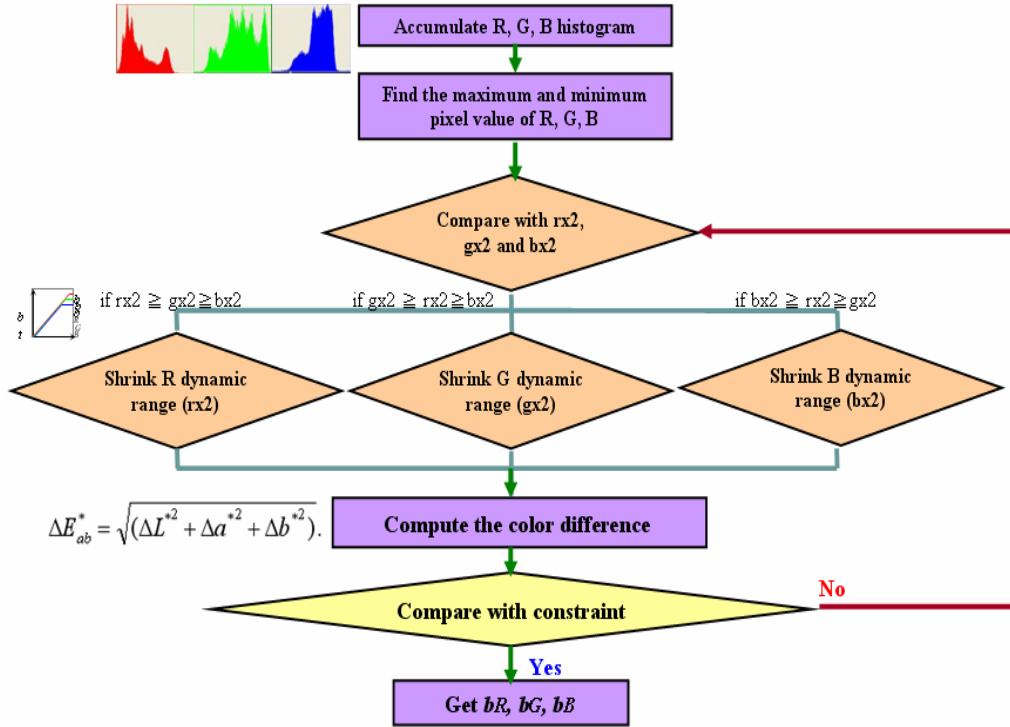


Figure 5-2. Procedure of finding backlight factor.

5.2 Luminance Scaling

The original CBCS algorithm [10] is used in the second phase. The affined linear transformation of a pixel p_L can be parameterized by

$$CBCS(gl, 0, gu, b_L) \equiv p_L^* = \begin{cases} 0, & p_L < gl \\ c(p_L - gl), & gl \leq p_L \leq gu \\ b_L, & gu < p_L \end{cases} \quad (5-2)$$

where b_L is the backlight factor and

$$c = \frac{b_L}{gu - gl}. \quad (5-3)$$

The image quality is defined by

$$F_C = \sum_{gl}^{gu} f_c(x) PDF(x), \quad (5-4)$$

where

$$f_c(x) = \begin{cases} 0, & 0 \leq x < gl \\ c, & gl \leq x \leq gu, \quad 0 \leq c \leq 1 \\ 0, & gu < x \leq 1 \end{cases} \quad (5-5)$$

and $PDF(x)$ is the probability density function of pixel value x . The RGB backlights are scaled simultaneously by a factor b_L such that no more color shift will be introduced. Since the ratio between the RGB is fixed, this phase is called luminance scaling. The following LED power equation is used.

$$P_R(b_L b_R) + P_G(b_L b_G) + P_B(b_L b_B) \quad (5-6)$$

The objective function is to find the optimal gl , gu , and b_L that minimize Equation (5-6) subject to the given image quality constraint F_C .

Sample transfer functions of chromaticity and luminance scaling are shown in Figure 5-3.

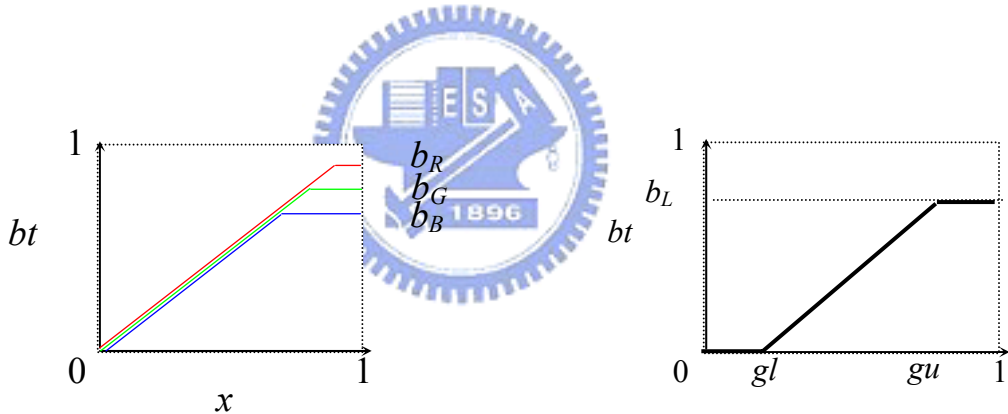


Figure 5-3. Transfer functions of chromaticity and luminance scaling.

5.3 Summary

In our algorithm, the chromaticity scaling is employed to find the maximum power consumption which can be saved in an image while the color difference ΔE is determined. We reduce the backlight intensity by using the results of chromaticity scaling.

Luminance scaling uses CBCS algorithm. The transfer function changes the pixel data for compensating the luminance loss while the backlight intensity is reduced. The algorithm is the foundation that constructing a platform of the low power display.

Chapter 6

Prototype

6.1 Framework

For implementing our algorithms of backlight scaling, a prototype of experimental platform is necessary. Unfortunately, it is too difficult to get an appropriate hardware for matching the portable electronic device. Furthermore, the structure and optical mechanism of the portable electronic device can be easily shifted or damaged after the panel refitted. Therefore, it is critical to determine a prototype to overcome these difficulties.

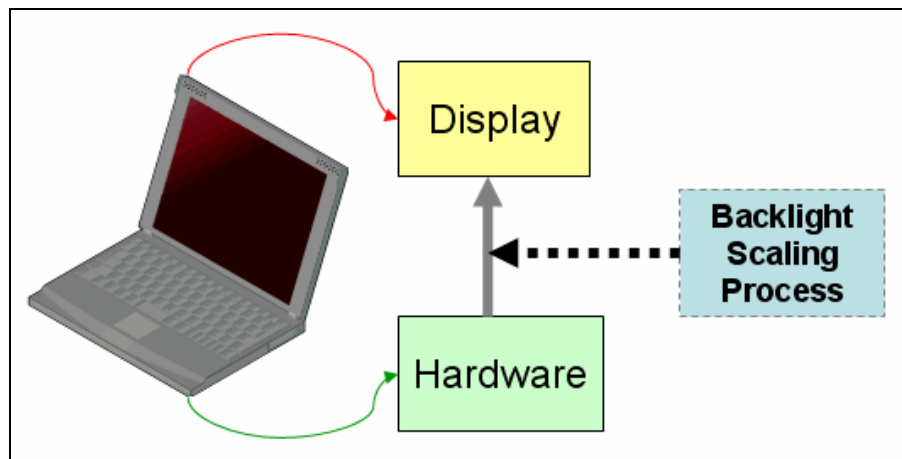


Figure 6-1. Backlight scaling of portable electronic device.

The design of our prototype is changed from the portable electronic device system (small size panel) to the laptop computer system (large size panel) through the support of CPT Corporation. Because our purpose is to reduce the power consumption of the TFT-LCD backlight, this switch has no influence on our implementation. There are several benefits in this switch. A ready hardware (FPGA board) from the support of CPT Corporation can be used to design this prototype. Refitting the large size panel is easier than refitting the small ones for us. Moreover, for a panel manufacturer, they can apply the technology of large size

panel to the small size panel readily. The power consumption of the LCD backlight can be measured more conveniently.

In our framework, the backlight scaling algorithm is realized in a Field Programmable Gate Array (FPGA) board. The FPGA board is used for image processing and backlight controller, which connects the TFT-LCD and the personal computer. The TFT-LCD displays the images before/after the backlight scaling process with the FPGA, while we measure the power consumption of TFT-LCD backlight.

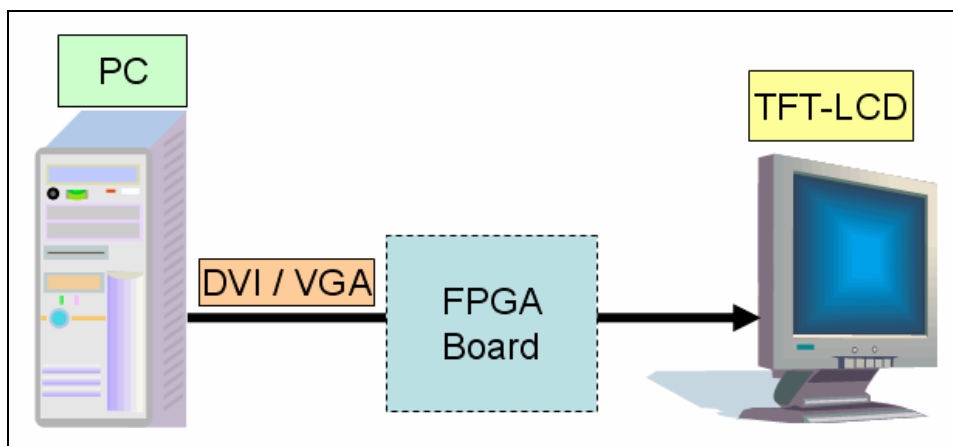


Figure 6-2. Our notion of backlight scaling.

6.1.1 Image Processing Flow

In image data processing flow of the personal computer, first, the image data is stored in the frame buffer by the CPU, and then graphic card fetches this image data and generates appropriate analog or digital image data to the video interface. The image data is carried by VGA or DVI interface and delivered to the scaler board.

According to the panel characteristic, the scaler board automatically scales the image data to appropriate frame resolution and frame rate. Moreover, some scaler chips include extra functionality, such as video decoding, video processing and 3D graphics accelerator, etc. Finally, the image data is translated into the signal format of TTL or Low Voltage Differential Signaling (LVDS) by scaler board and is delivered to panel controller board.

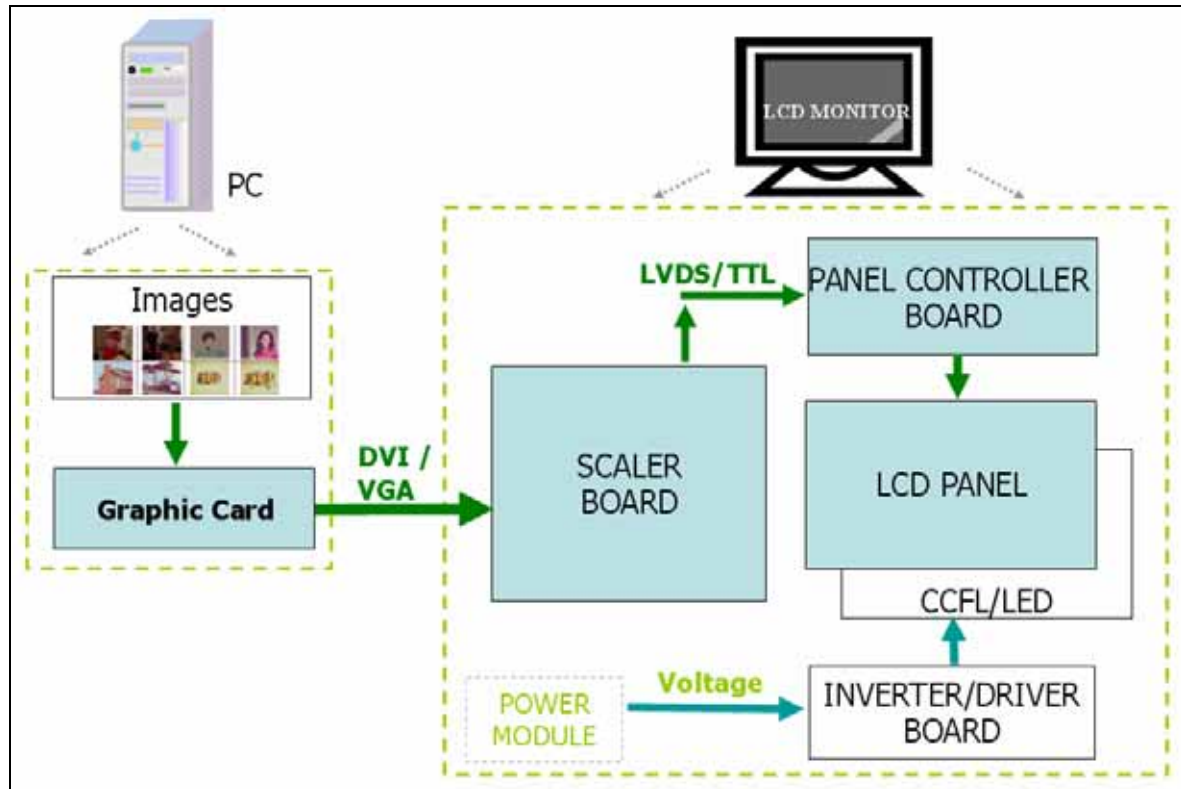


Figure 6-3. Block diagram of image processing flow.

6.2 Block Diagram of Prototype

Our goals are to reduce the power consumption of the LCD backlight and to maintain the image brightness with our backlight scaling algorithms. This consideration of fetching and processing image data from the PC will be used to design the experimental platform. There are different methods available to fetch the image data; one is to fetch the image data as it is delivered by graphic card, and another is to fetch the image data as it passes the scaler board.

It is more complex to process image data with the first method. Furthermore, some scaler boards include the functionality of image processing. While the image data passes the scaler board, the image data is probably adjusted or changed by scaler board. Base on the above reasons, we chose the second method. Unfortunately, because of the higher resolution TFT-LCD panel, the image data is translated into LVDS signal format by the scaler board while the image data passes the scaler board. LVDS signal format will complicate the image

fetching and processing.

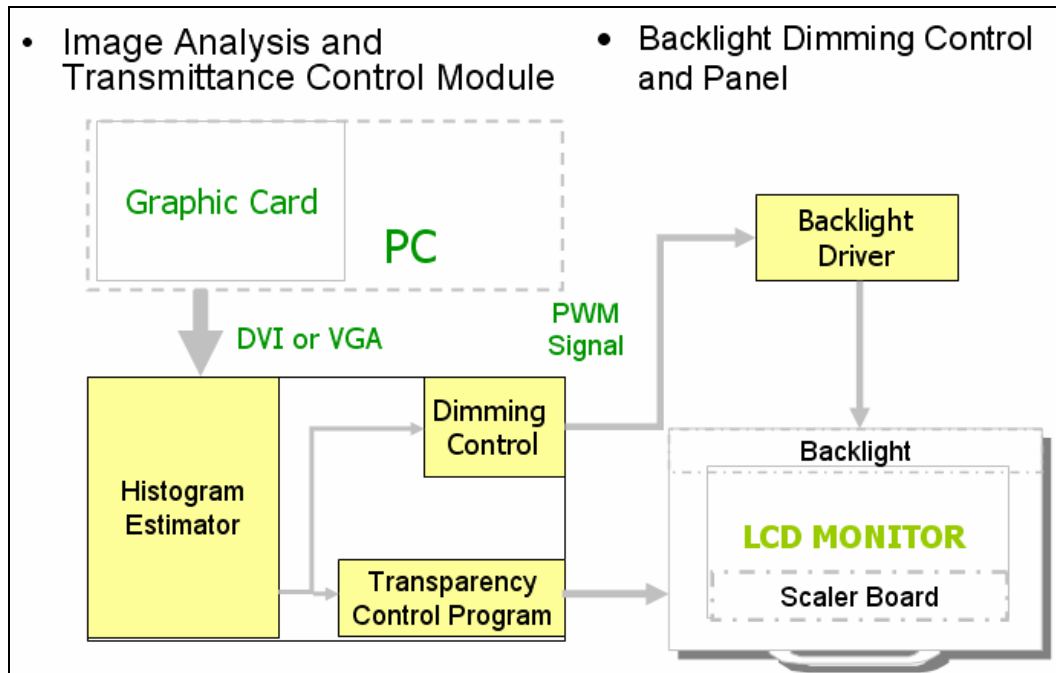


Figure 6-4. Fetching the image data as the image data is delivered by graphic card.

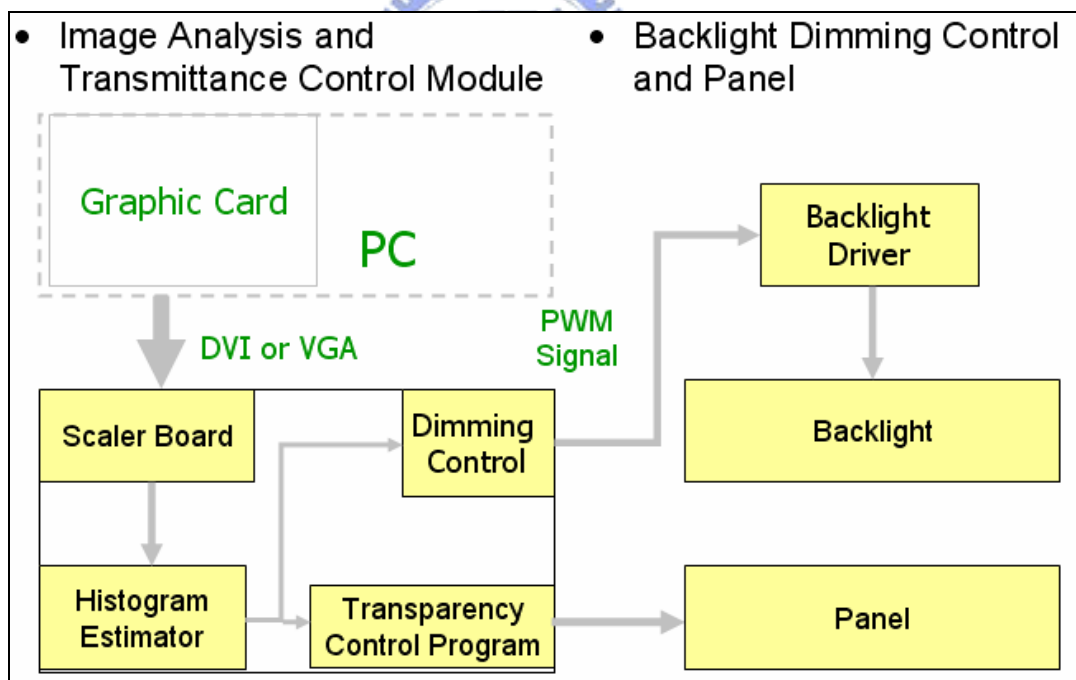


Figure 6-5. Fetching the image data as the image data passes the scaler board.

6.2.1 Low Voltage Differential Signaling

The signal format of LVDS is a technology addressing the needs of today's high

performance data transmission applications. The LVDS standard is becoming the most popular differential data transmission standard in the industry.

In the TFT-LCD field, the LVDS standard is usually used in the signal transmission of the higher-resolution LCD because it requires more data flow than low-resolution LCD.

LVDS delivers high data rates while consuming significantly less power than competing technologies. In addition, it brings many other benefits, which include:

- Low-voltage power supply compatibility
- Low noise generation
- High noise rejection
- Robust transmission signals
- Ability to be integrated into system level ICs

LVDS technology allows products to address high data rates ranging from 100's of Mbps to greater than 2 Gbps. For all of the above reasons, it has been deployed across many market segments wherever the need of speed and low power exists.

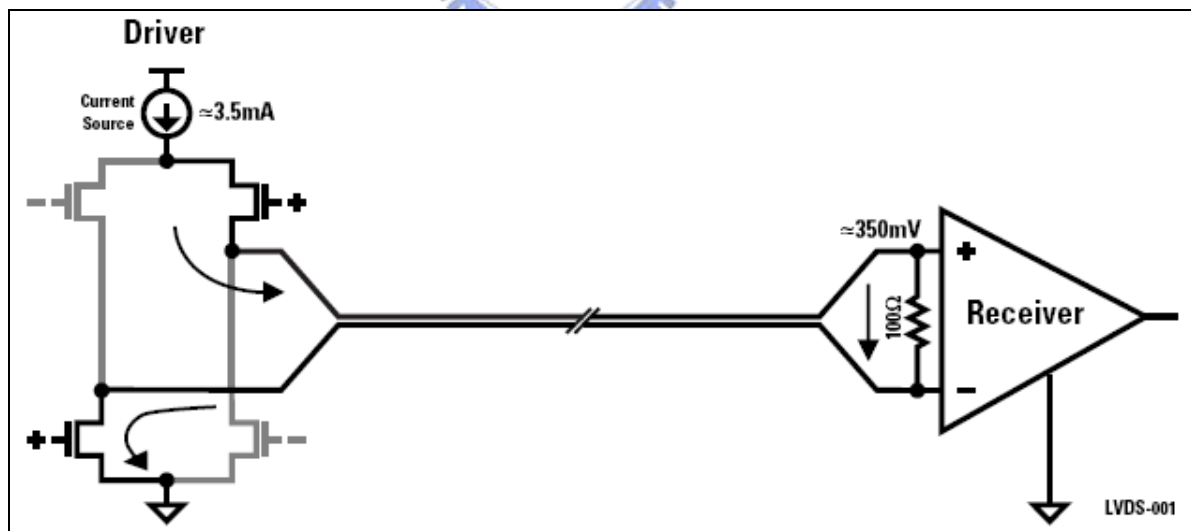


Figure 6-6. Simplified diagram of LVDS driver and receiver.

LVDS is a low swing, differential signaling technology, which allows single channel data transmission at hundreds or even thousands of megabits per second (Mbps). Its low swing and current-mode driver outputs create low noise and provide very low power consumption across

a wide range of frequencies.

LVDS outputs consist of a current source (nominal 3.5 mA) that drives the differential pair lines. The basic receiver has a high DC input impedance, so the majority of driver current flows across the 100 Ω termination resistor generating about 350 mV across the receiver inputs. When the driver switches, it changes the direction of current flow across the resistor, thereby creating a valid “one” or “zero” logic state.

6.3 Platform

6.3.1 Experimental Panel

The experimental panel is equipped with a 1280 \times 1024, 19”, 24-bit color, transmissive, color TFT-LCD monitor, ViewSonic VX912.

In our work, LED was used to fabricate backlight module. The backlight scaling panel and backlight was evaluated by a conventional TFT-LCD monitor. The prototype was built on a VX912 monitor. Originally the LCD panel has two side-lit CCFL backlights on the top and bottom. We custom made two LED backlights to replace the CCFL backlights.

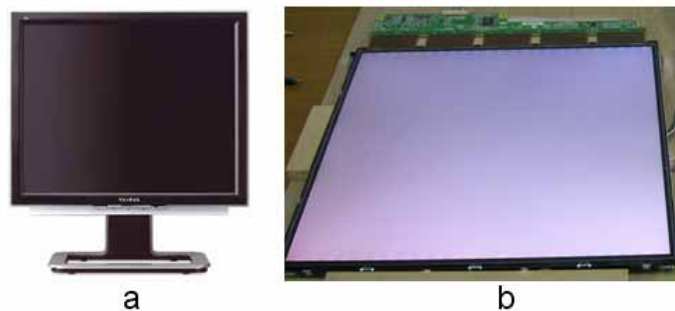


Figure 6-7. VX912 monitor and panel.

The display panel manufactured by AUO Corporation includes a major application specific integrated circuit (ASIC) and an SXGA TFT-LCD panel [30]. The image data feeds into the AUO ASIC, which includes the timing controller and RSDS transmitter. The connector receives the LVDS signal which is from the scaler board, and then delivers to the AUO ASIC. The LVDS signal is translated into RSDS by the AUO ASIC, and then delivers to TFT-LCD. The LVDS signal is translated into RSDS by the AUO ASIC, and then delivers to TFT-LCD.

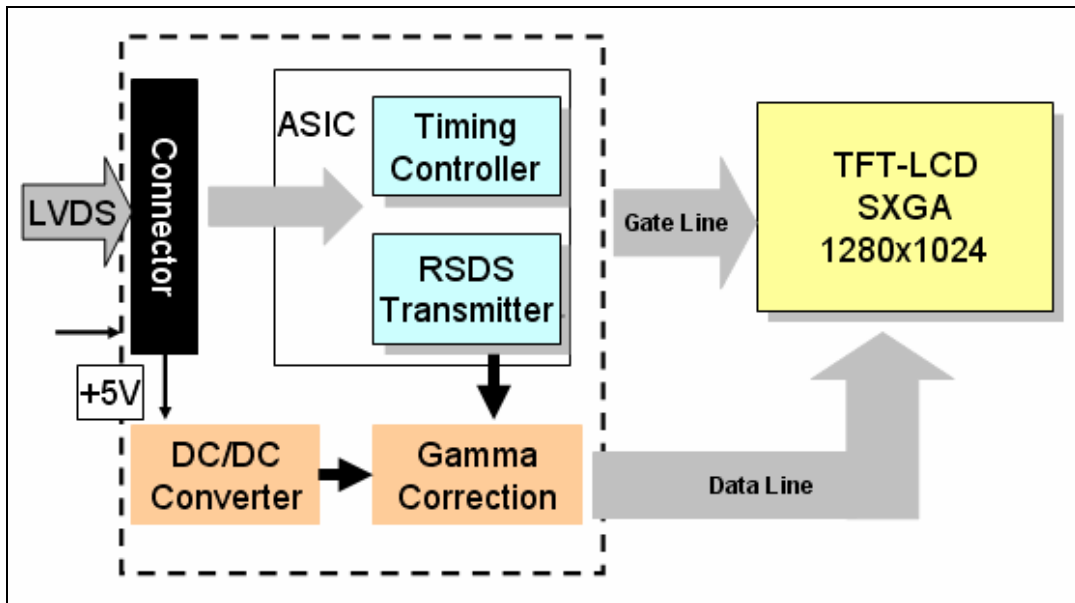


Figure 6-8. Block diagram of the AUO panel.

6.3.2 FPGA Board

In the beginning, we implement the panel controller and backlight controller with an FPGA board which is supplied by CPT Corporation and Xilinx Spartan-3 Starter Kit [31], respectively. The CPT FPGA board includes an LVDS transmitter and receiver, and an FPGA chip. The Xilinx Spartan-3 starter kit houses 200,000-gate Xilinx Spartan-3 XC3S200 FPGA in a 256-ball thin ball grid array package (XC3S200FT256), 2Mbit Xilinx XCF02S platform flash, in-system programmable configuration PROM, 1M-byte of fast asynchronous SRAM, 3-bit, 8-color VGA display port, 9-pin RS-232 serial port, 50 MHz oscillator, and several I/O ports.

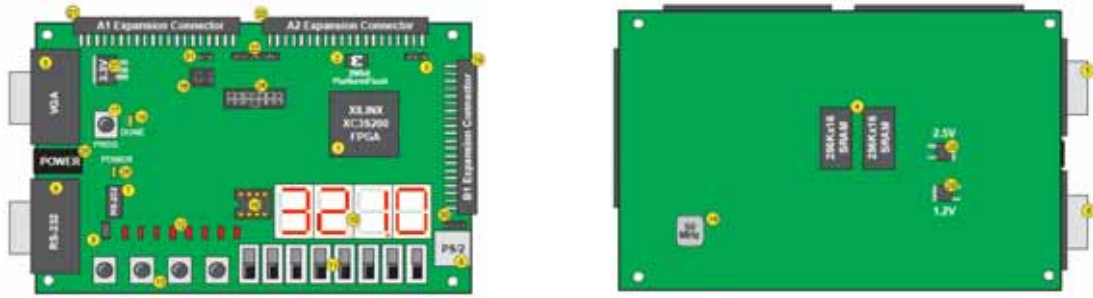
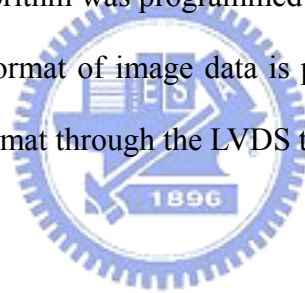


Figure 6-9. Xilinx Spartan-3 Starter Kit Board [31].

The CPT FPGA board includes three major ports; they are LVDS receiver, FPGA chip, and LVDS transmitter. The function of the LVDS receiver is to translate the LVDS signal format of image data to TTL signal format. Next, the TTL signal is delivered to the FPGA chip.

Our backlight scaling algorithm was programmed in HDL code, and then written into the FPGA chip. The TTL signal format of image data is processed by the FPGA chip, and then translated into LVDS signal format through the LVDS transmitter.



6.3.3 LED backlight

Our prototype LED backlight uses top-emitting LED chips. Each LED chip houses four LEDs – one red, two green in series, and one blue. The 1:2:1 ratio was determined by chromatic sensitivity and device efficiency. The three colors were driven separately such that the output chromaticity can be adjusted.

The LED backlights were used to replace the CCFL backlights of the VX912. Each LED backlight consists of 24 LED chips, wired as 4 parallel sets of 6 serial chips. Each channel is driven by a dedicated current mirror driver on a custom designed PCB. The driving current is controlled by a pulse-width modulation (PWM) signal.



Figure 6-10. LED and LED backlight.

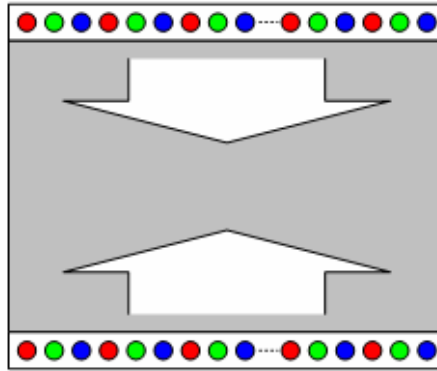


Figure 6-11. Block diagram of backlight module.

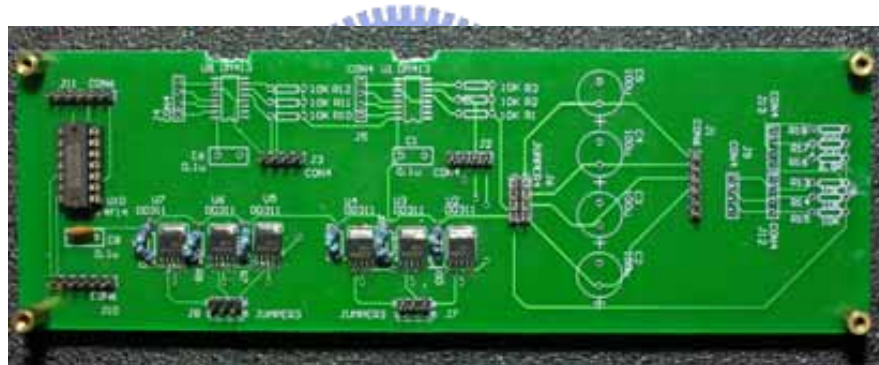


Figure 6-12. LED backlight driving board.

6.3.4 Instruments and Equipment

The color and brightness of image are the most important properties of a system that we want to evaluate. The chroma meter (Konica-Minolta chroma meter CS-200) was used to measure these properties. It utilizes three high-sensitivity silicon photo-cells, which are filtered to match the CIE standard observer response. It can be used to measure various chromaticity coordinates by calculating three measurements, such as L_{xy} , L_{uv} , $L_{u'v'}$, dominant wavelength, color temperature, etc. With this compact, reliable color analyzer, we

can easily get the chromaticity coordinates and luminance of the displayed image. The chroma meter CS-200 was also used to calibrate the white point of our prototype.

The programmable power supplies, GW PPT-3615, were used to support the LED driving board and LED backlights power. The digital multimeters, GDM 8246, were used to measure the current of LED backlights. We can obtain the voltage data of the LED backlights from the power supplies, and also obtain the current data from the multimeters. The power consumption can be calculated as the product of the voltage and current.



Figure 6-13. Chroma meter.



Figure 6-14. Power supply.



Figure 6-15. Multimeter.

6.3.5 Platform Block Diagram

In the final block diagram, we combined the backlight controller and panel controller onto the CPT FPGA board. The algorithm was also implemented in VHDL, the CPT FPGA Board. The following block diagrams are illustrated around the experimental setup in Figure 6-16.

- PC: Generating the image signals for the scaler board.
- Scaler Board: Scaling the image data to appropriate frame resolution and frame rate where the image signal is LVDS format.
- FPGA Board: Receiving LVDS signals and then translating signal to the TTL format. Furthermore, performing the proposed algorithm image processing, and then outputting the VGA signal to drive the 19" TFT-LCD panel. At the same time, The FPGA board also generates the pulse width modulators (PWM) to control the

backlight intensity of the RGB channels.

- Multimeter: Measuring the driving current of the LEDs.
- Power Supply: Powering LED and their drivers.
- LED Driver: Driving the LEDs.

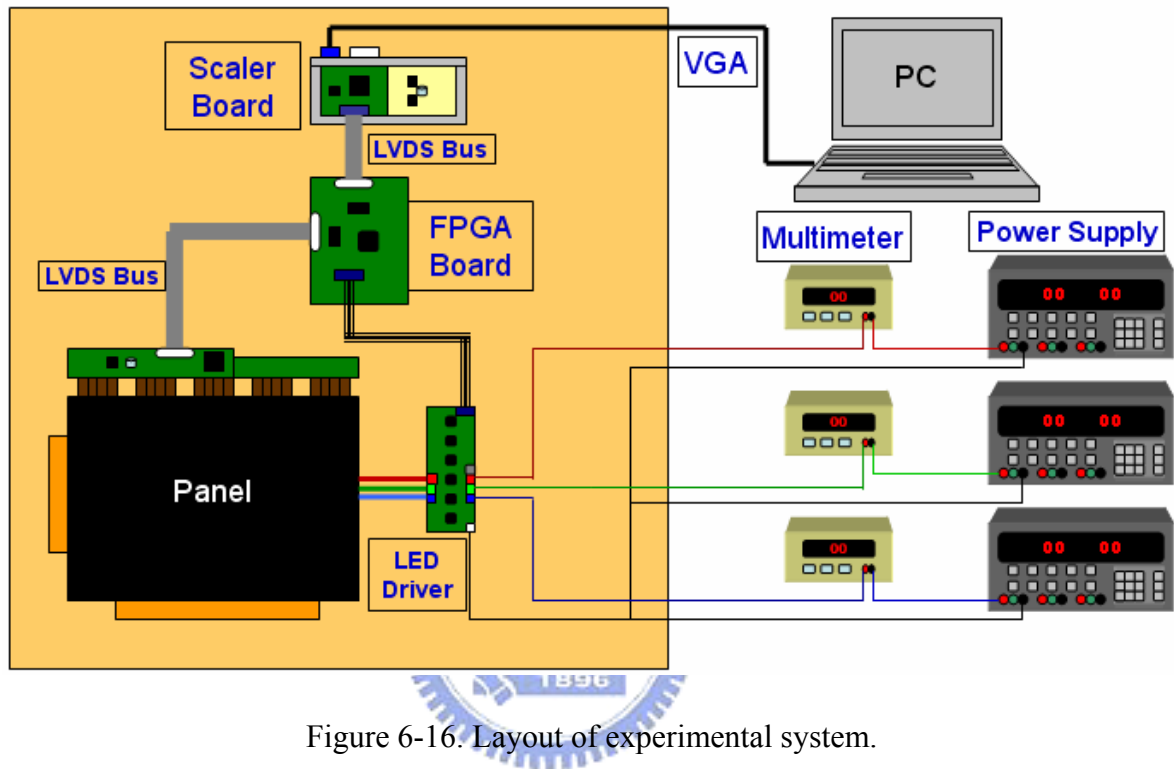


Figure 6-16. Layout of experimental system.

6.4 FPGA Architecture

The critical component of our experimental platform is the CPT FPGA board. The algorithm of backlight scaling is programmed with very high speed integrated circuit hardware description language (VHDL) code and then writes into the FPGA chip, which is on the CPT FPGA board. The two major assignments are executed by FPGA chip adjust the image data from the scaler board and adjust the backlight intensity.

6.4.1 Display Signal

The display signal plays a decisive role in programming HDL code. CRT display is based

on an afterimage of human eyes. As we reduce the refresh rate of the CRT display that exceeds the minimum period for an afterimage on the human eye, we start to feel flicker. In other words, the image on the CRT display is always flickering; but human eyes do not recognize it as long as the flickering frequency is high enough. Meanwhile, the image on the TFT LCD panel also flickers, but the flicker on the LCD panel is of a different nature. As far as the refresh rate is higher than the time constant of the storage capacitors, the image on the LCD display does not flicker at all. Consequently, we can reduce the refresh rate of the LCD display as long as it is shorter than the time constant of the storage capacitors. Actually, modern LCD displays adopt flicker free techniques, and the time constant is much longer than that of the CRT display. In addition, as we increase the refresh rate of the CRT display far exceeding the minimum period for the afterimage, we do feel better quality; so we often use 120Hz or higher refresh rate for high quality image. However, once the refresh rate is higher than the time constant of the storage capacitors, the image quality of the LCD display is not enhanced further. Therefore, most LCD panels support fixed refresh rate, unlike CRT displays.

Vertical synchronization (Vsync) is a signal used to describe the process or set a value telling the monitor when to draw the next vertical line. Vsync determines the frame frequency of the display. The frame rate of CRT display can be adjusted, but LCDs cannot, due to the LC response time is limited. So, most LCDs support fixed frame rate, unlike CRT display. Meanwhile, the frame rate of the TFT-LCDs is usually 60Hz. Horizontal synchronization (Hsync) is a signal telling the monitor to stop drawing the current horizontal line, and starts drawing the next line. Each high state of the DE (data enable) signal matches the high state of a Hsync signal.

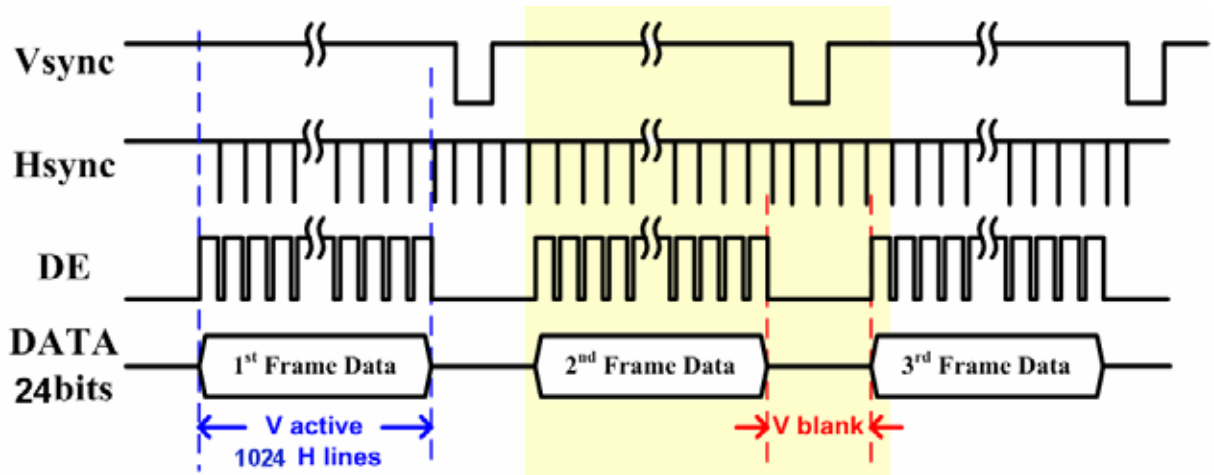


Figure 6-17. Waveform chart of video signal (a).

The DE signal determines the data writing in the period of the high state. In the period of high state of the DE signal, which is active time and the data of an image is valid. As the DE signal is low state, the data of the image is invalid even though the Hsync is high state.

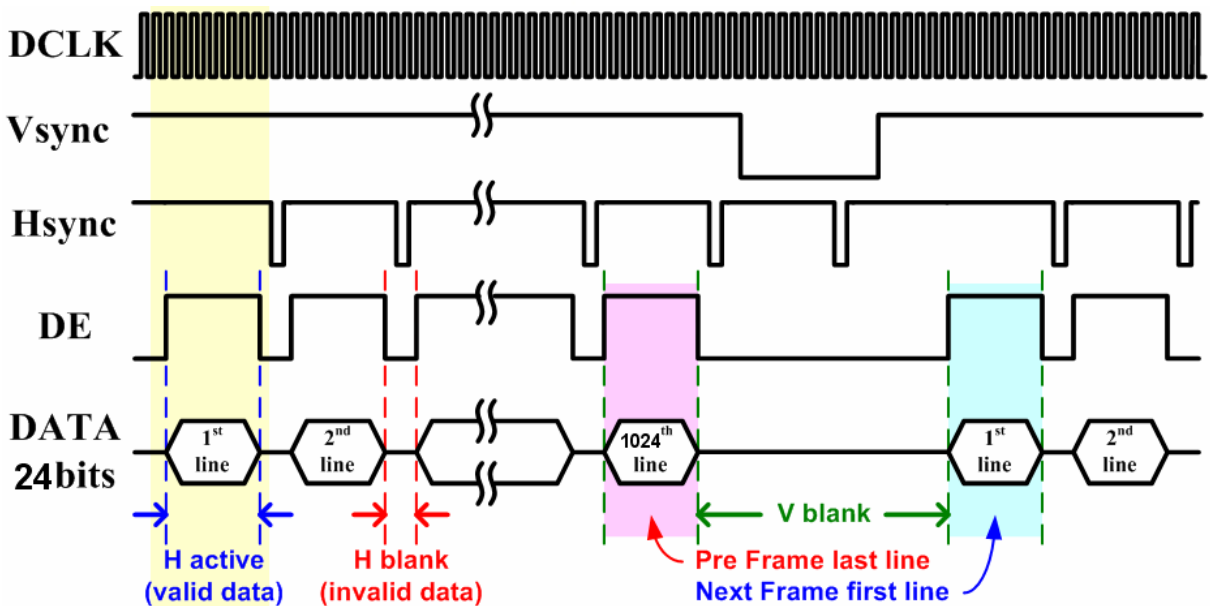


Figure 6-18. Waveform chart of video signal (b).

The DCLK means the pixel clock. Each period of the DCLK represents the transmission data of a pixel is valid and the amount of the pixels is 1280 while the DE is high state. Meanwhile, the data width is 24 bits, which means that the data width of R, G, and B of an image has 8 bits.

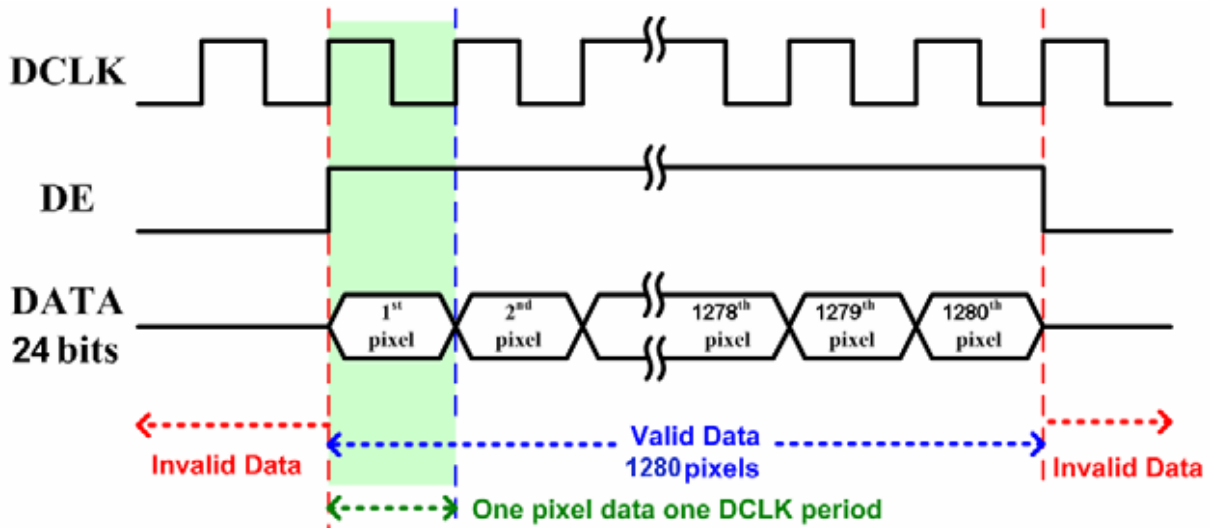


Figure 6-19. Waveform chart of video signal (c).

6.4.2 LVDS Interface / TFT Data (Color) Mapping

Different color mapping options exist. The LVDS clock wave shape is shown in Figure 6-20. The rising edge of the LVDS clock occurs two LVDS sub symbols before the current cycle of data. The clock is composed of a 4 LVDS sub symbol HIGH time and a 3 LVDS sub symbol LOW time. The respective pin (transmitter and receiver) names are shown in Figure 6-20. As stated above, these names are not the color mapping information (MSB/LSB), but the pin names only.

In Figure 6-20, inputs B17 and B27 are double width. In the LVDS receiver IC, these bits are sampled in the back half of the bit only. Also, the DE signal is mapped to two LVDS sub symbols. The LVDS receiver IC only samples the DE bit on channel A2.

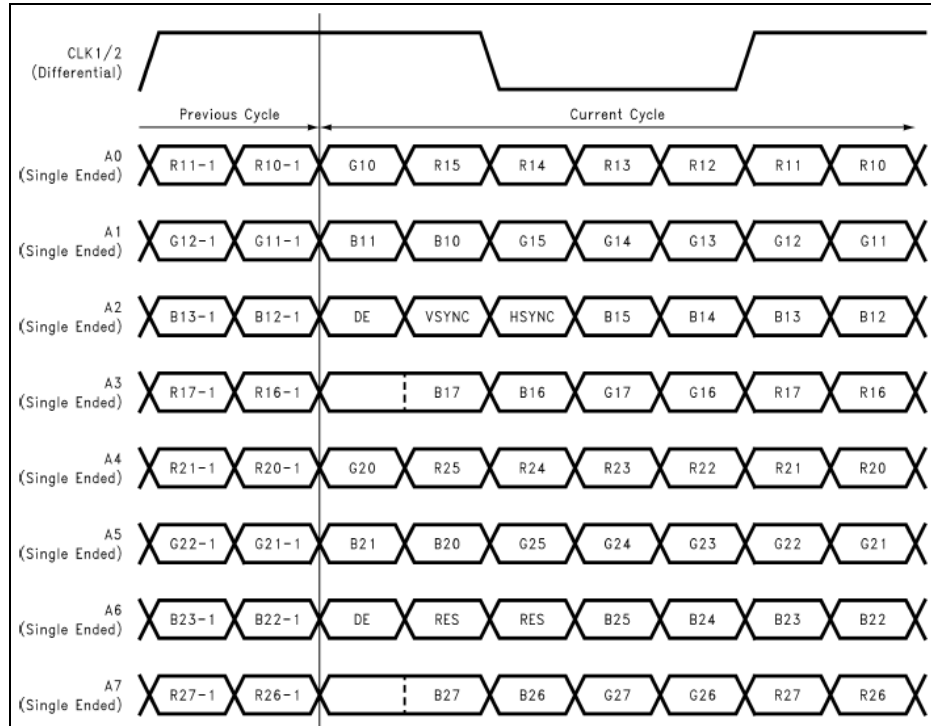


Figure 6-20. TTL data inputs mapped to LVDS outputs [32].

6.4.3 Implementation of Algorithm

The basic hierarchy of the FPGA is shown in Figure 6-21. The LVDS signal, which is from scaler board, is translated into TTL signal by the LVDS receiver of CPT FPGA board and then is delivered to FPGA chip. In our process flow, first, each frame is stored with his image data. Next, we calculate the clipping boundary of the histogram by our algorithm. The two blocks of backlight adjusting hierarchy and transmittance adjusting hierarchy employ the clipping boundary as the parameter for the image process based on our backlight scaling algorithm to calculate the pixel transfer function for the original image. Finally, the original image data is translated into scaling image data by transmittance adjusting hierarchy and then is delivered to LVDS transmitter. The LVDS transmitter translates the TTL signal into LVDS signal and then delivers the LVDS signal to the TFT-LCD panel. At the same time, the PWM signal delivered to the LED backlights from backlight adjusting hierarchy for dimming the LED backlights.

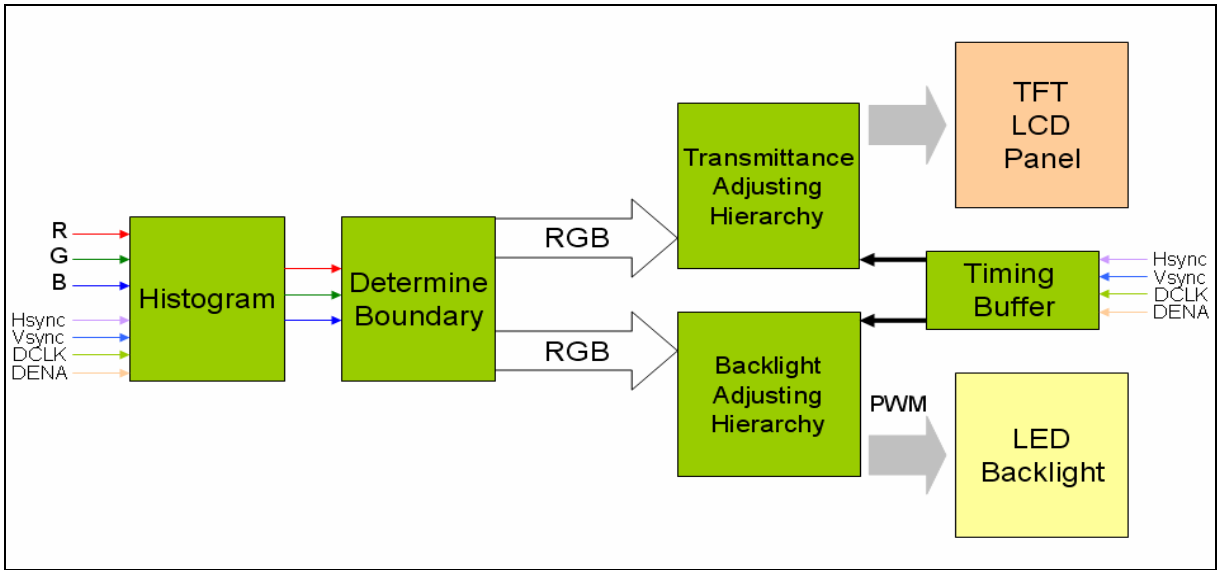


Figure 6-21. Basic hierarchy of the HDL code.

Histogram Calculation

Because of the memory issues of the FPGA chip, we divided the histogram of the image data into four bins. There are totally 256×3 registers to count the number of image data of a pixel. We program a dynamic RAM with the FPGA chip and store the statistics of these registers in the dynamic RAM.

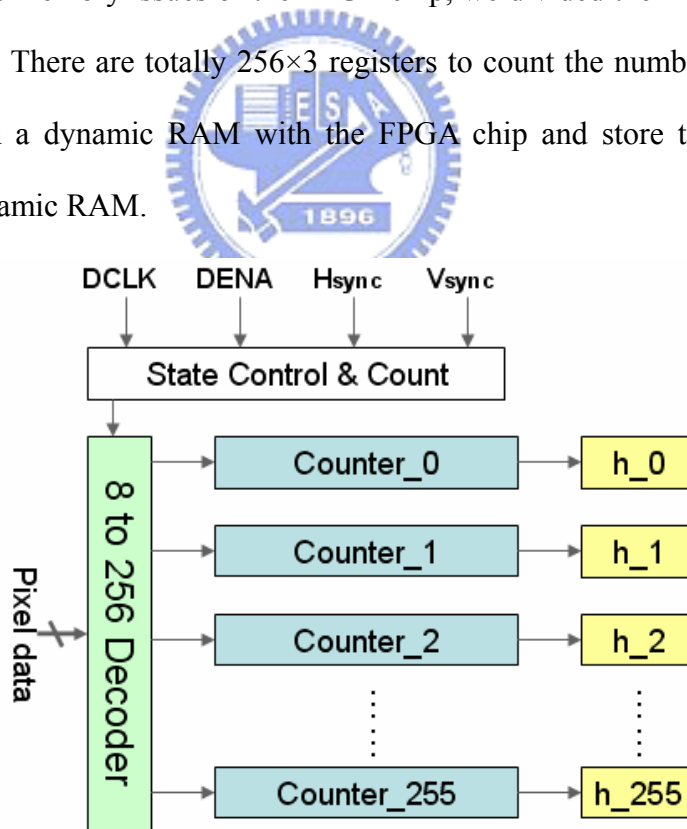


Figure 6-22. The histogram calculation module.

There are three histogram calculation modules for RGB channel. Each gray value of the 256 values is used as an input for the 8 to 256 decoder shown in Figure 6-22 to determine

which of the 256 counters will be incremented. The counters Counter_0 to Counter_255, illustrated in the figure, are used to determine the number of pixels utilizing each gray level. The value of each counter is stored in a register hi , where $i = 0, 1, 2, \dots, 255$ is the corresponding gray value. At this point, the histogram values for all of the gray levels are obtained.

Determine Boundary

In our algorithm, it requires a large number of the calculation to determine these clipping boundaries. The implementation of the FPGA is difficult due to the logic gate of the FPGA chip is limited and the code of HDL is very complex. Furthermore, lots of the calculation also causes serious timing delay.

Due to the transmission speed of the image signal of the SXGA panel is very fast, the influence of the timing delay cannot be neglected. For example, two identical signals from the scaler board input the FPGA chip at the same time, one signal which passing through the longer path in the FPGA chip has more serious timing delay than the other which passes through the shorter path in the FPGA chip. The two different timing delays between the signals will cause the signals are not synchronous and then the LCD displays the wrong image. The Lookup table (LUT) is created and used to overcoming that the timing delay and number of the logic gate issues. The determine boundary block will generate corresponding data according to the LUT while the histogram data delivers to this block.

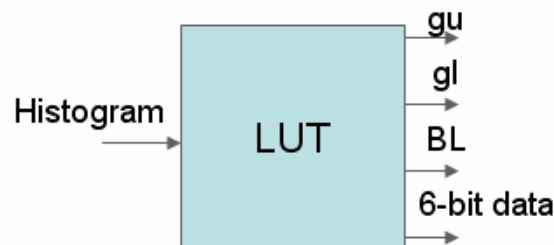


Figure 6-23. The boundary determination block.

Backlight adjusting hierarchy

The backlight adjusting hierarchy is used to determine the PWM signal through the data from the above block. The backlight adjusting hierarchy includes three major units, the data registers, PWM signal generators and timing adjusted unit. In the beginning, the data is stored in the data registers, and then the PWM generators determine the duty cycle of the output signal according to the data of the registers. Next, the PWM signal is delivered to timing adjusted unit. The timing adjusted unit is enabled by timing buffer, and the PWM Generator will deliver the PWM signal to the LED backlights. The intensity of the LED backlights will be determined by the PWM signal.

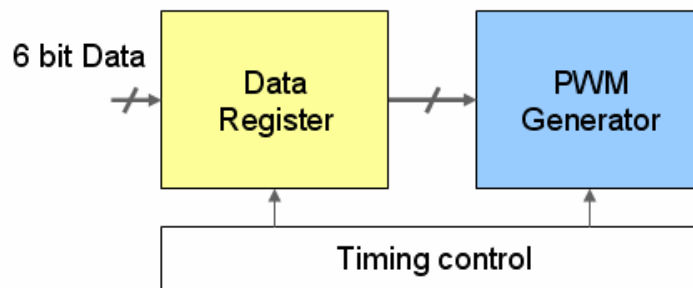


Figure 6-24. The circuit scheme of backlight adjusting hierarchy.

The PWM Generator is composed of a 6-bit counter and a 6-bit unsigned comparator shown in Figure 6-25. The duty cycle of the PWM signal depends on the Data_in. The output of the comparator is high while C_in is smaller than Data_in.

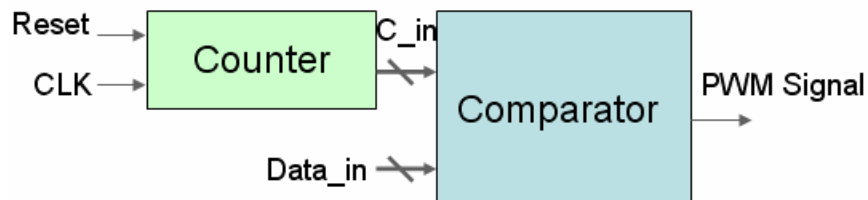


Figure 6-25. The PWM Generator.

Transmittance adjusting hierarchy

The transmittance adjusting hierarchy is used to the transmittance of the panel. It

includes the registers, subtracts, multipliers, dividers, and timing control unit. The output results of every pixel are calculated according to the input data which is from the above block. The circuit scheme is shown in Figure 6-26. Due to the pixel data is unsigned, the process that eliminating negative value is necessary. The outputs of the comparators are used to make subtracts generate absolute value.

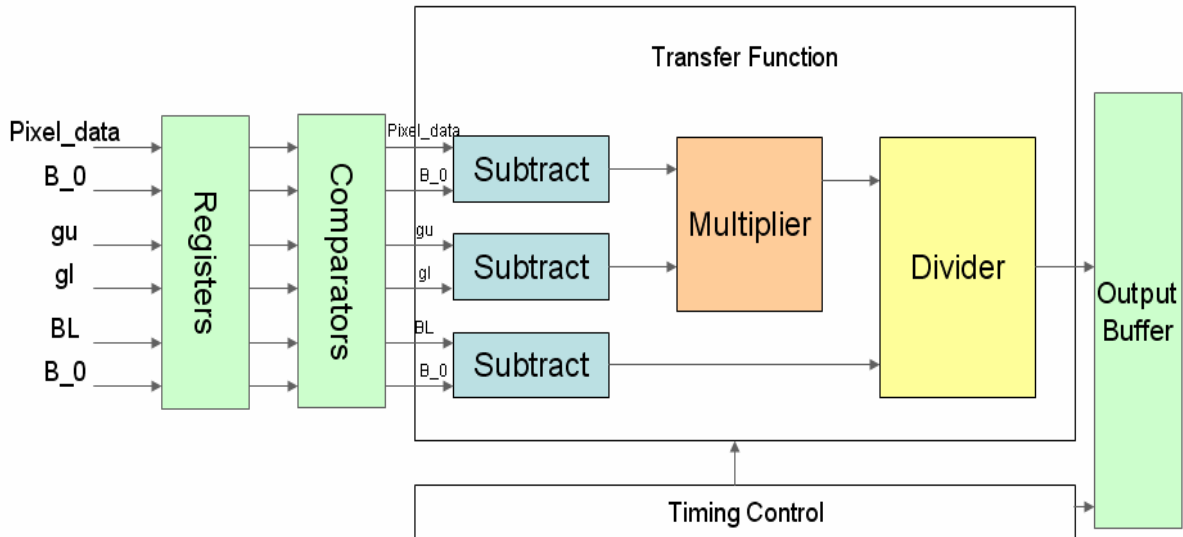


Figure 6-26. The circuit scheme of transmittance adjusting hierarchy.

In our luminance scaling algorithm, the transfer function will result in a floating decimal. In order to avoid computing the floating decimal and simplify the circuit, we finish the multiplication first, and then do division.

Timing Buffer

The timing buffer is composed of the flip-flop. This buffer is very important for synchronize the panel transmittance and LED backlight intensity. The timing buffer synchronizes the output of transmittance adjusting hierarchy and backlight adjusting hierarchy. If the variations of the LED backlight and panel are asynchronous, the observers will perceive the wrong image on this display.

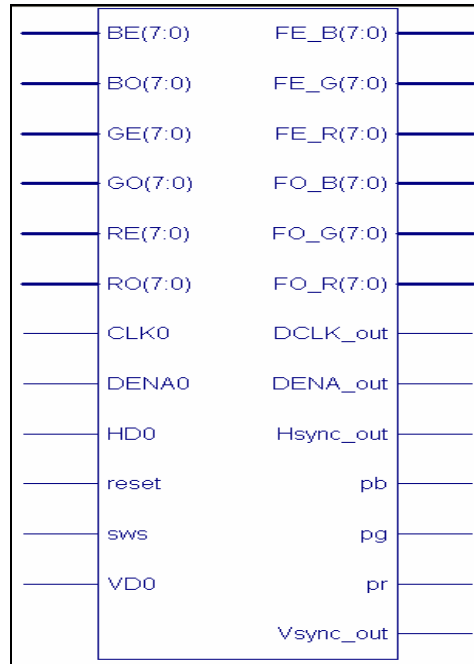


Figure 6-27. The block diagram of the FPGA chip.

Figure 6-27. shows the block diagram of the FPGA chip. The following description expresses the function of every pins of the FPGA chip.

- RE, GE, and BE: The inputs of the even line of the image data.
- RO, GO and BO: The inputs of the odd line of the image data.
- CLK0: The input of the pixel clock.
- DENA0: The input of the data enable.
- HD0: The input of the Hsync.
- VD0: The input of the Vsync.
- sws: The ON/OFF of the backlight scaling.
- reset: The image data reset.
- FE_R, FE_G, and FE_B: The outputs of the even line of the image data.
- FO_R, FO_G, and FO_B: The outputs of the odd line of the image data.
- DCLK_out: The output of the pixel clock.
- DENA_out: The output of the data enable.
- Hsync_out: The output of the Hsync.

- Vsync_out: The output of the Vsync.
- pr, pg, and pb: The output of the PWM signal for adjusting LED backlight intensity.

6.4.4 Hardware Cost

The hardware usage is shown in Table 6-1. The power consumption of the FPGA chip was analyzed with the software, Xpower. The total power consumption is 63mW. The total memory usage of the FPGA chip is 133208 kilobytes and the most serious delay time which is from source pad to destination pad is 14.939 ns.

Table 6-1. The FPGA chip usage.

Logic Utilization	Used	Available	Utilization
Total Number Slice Registers	126	15,360	1%
Number used as Flip Flops	120		
Number used as Latches	6		
Number of 4 input LUTs	1,648	15,360	10%
Logic Distribution			
Number of occupied Slices	1,058	7,680	13%
Number of Slices containing only related logic	1,058	1,058	100%
Number of Slices containing unrelated logic	0	1,058	0%
Total Number 4 input LUTs	1,735	15,360	11%
Number used as logic	1,648		
Number used as a route-thru	87		
Number of bonded IOBs	109	333	32%
Number of Block RAMs	3	24	12%
Number of GCLKs	6	8	75%

6.5 Summary

If the optical design for this panel can be implemented to our experimental platform, this

prototype design will be more complete. Unfortunately, the mechanism of the panel is fixed, to implement the optical design methodologies and technique is very difficult. However, the luminance uniformity of the panel is acceptable. The LED backlights possess larger color gamut. The color saturation of LED backlights is better than CCFL backlights.

In addition, the high resolution LCD such as the VX912, there are many considerations for programming the HDL code due to the pixel clock has higher frequency. Moreover, we don't have any information for the AUO ASIC; it also increases the difficulty for the FPGA design. Whatever, we overcome these design difficulties and finish the simple experimental platform.

The experimental setup is shown in Figure 6-28. As mentioned before, we introduce our experimental system. Our algorithm has been used by related projects to compute the necessary compensation of the image. However, the results are simply validated through our experimental system. We can control the image data from the PC and the LED backlights. The LED backlight intensity is dimmed with CLS algorithm. On the other hand, the image brightness is compensated with luminance transfer function. The two scaling are implemented with using the CPT FPAG board. The total experimental platform design can be applied to small size panel system.

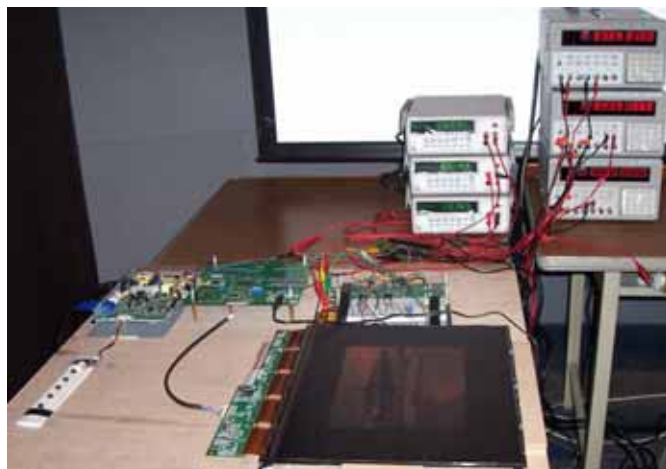


Figure 6-28. Experimental setup.

Chapter 7

Measuremental Results

In this chapter, we performed the power measurement on the panel of VX912 and our LED backlights. First, we measured the LCD component power consumption characteristics, and then we measured the power consumption while the algorithm of backlight scaling was applied to our LCD platform.

7.1 Hardware characterization

7.1.1 Panel

The hydrogenated amorphous silicon (a-Si:H) is commonly used to fabricate the TFT in display applications. For a TFT-LCD panel, the a-Si:H TFT power consumption can be modeled by a quadratic function of pixel value $x \in [0,1]$

$$P_{TFTpanel}(x) = ax^2 + bx + c \quad (7-1)$$

The VX912 is a normally-white TFT-LCD panel, which consumes less power while displaying brighter image. Thus, this type of panel adds additional power savings to the backlight scaling techniques because it generally enhances the luminance of the image that is displayed on the panel to compensate for the loss of the brightness after backlight dimming. In contrast, power consumption of a normally-black TFT-LCD panel increases slightly as its global transmittance increases, which increases power savings of a backlight dimming approach. However, in either type, the change in power consumption as a function of the transmittance is so small that it can be ignored.

We performed the current and power measurements on the LCD panel of VX912. The measured data are shown in Figure 7-1. The regression coefficients are thus determined as:

$$a=0.4737, b=-1.2046, \text{ and } c=4.9492.$$

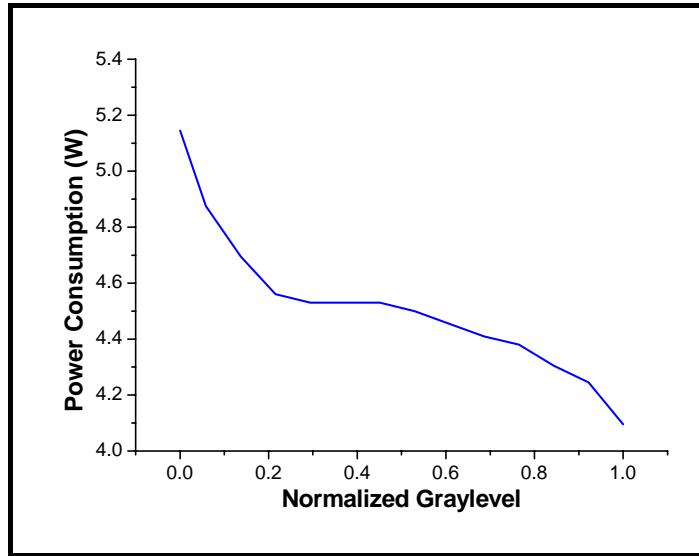


Figure 7-1. Pixel transmittance versus power consumption of a pixel in the normally white TFT-LCD panel.

7.1.2 LED backlights

We set the color temperature at 6500°K after the LED backlight was mounted onto the TFT-LCD panel, and then performed luminance and power characterization. The colorimetric data were measured by a Konica-Minolta CS-200 chroma meter. The power consumption vs. PWM duty cycle characteristics of LEDs are shown in Figure 7-2. The luminance vs. PWM duty cycle characteristics of the whole panel system are shown in Figure 7-3.

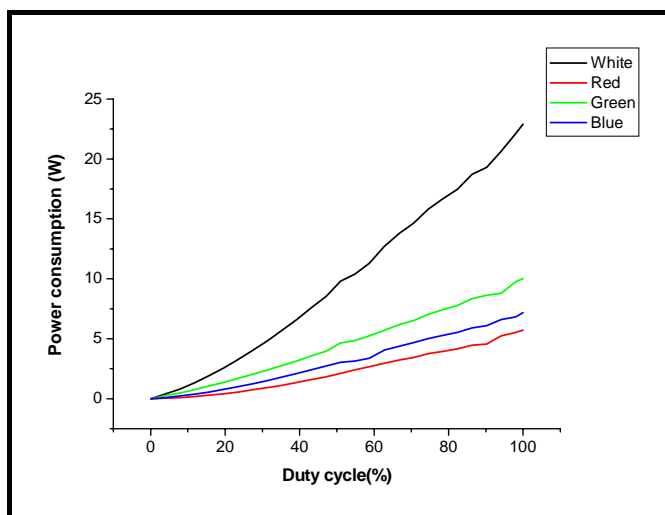


Figure 7-2. Power consumption vs. PWM duty cycle.

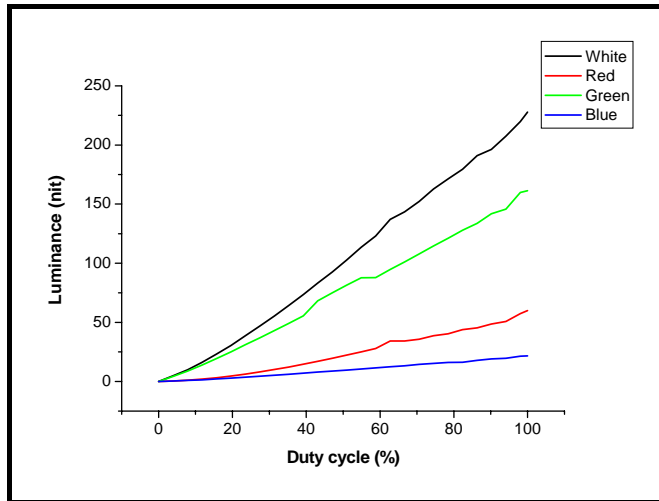


Figure 7-3. Luminance vs. PWM duty cycle.

Based on the measurement data, the luminance vs. power relation of LEDs can be modeled by polynomial functions as follows.

$$\begin{aligned}
 P_R &= 8 \times 10^{-5} b_R^2 + 0.0929 b_R - 0.0075 \\
 P_G &= 5 \times 10^{-5} b_G^2 + 0.054 b_G - 0.0284 \quad (\text{Watt}), \\
 P_B &= 0.0012 b_B^2 + 0.3102 b_B - 0.0951
 \end{aligned} \tag{7-1}$$

where b_R , b_G , and b_B are luminances of red, green, and blue backlight, respectively.

7.2 Results and discussion

Our algorithm was implemented through programming VHDL on an FPGA board, the CPT FPGA Board. This prototype receives DVI or VGA signal, performs the proposed backlight scaling image processing, and then outputs the signal to drive the 19" TFT-LCD monitor. At the same time, the FPGA board also generates the pulse width modulators (PWM) to control the backlight intensity of RGB channels. The photographs in Figure 7-4 show the side-by-side comparison between the prototype LED backlight and the original CCFL backlight monitor. After chromaticity scaling, the red, green, and blue channels are scaled down to 0.9, 0.8, and 0.7, respectively. The results of luminance scaled to 1.0 (unchanged), 0.8 (degraded), and 0.6 (unacceptable) are shown.

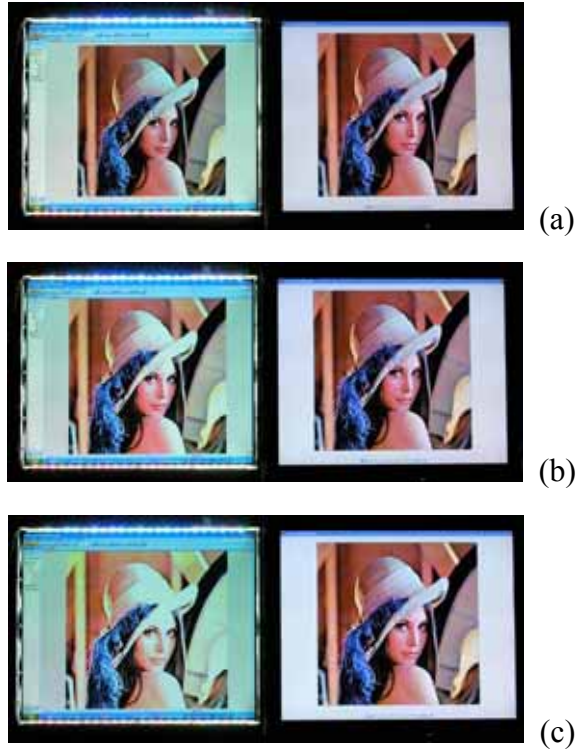


Figure 7-4. Photos of prototype LED backlit (left) and CCFL-lit (right) system, where $b_R=0.9$, $b_G=0.8$, and $b_B=0.7$. From top to bottom: $b_L=1.0$, 0.8, and 0.6.

The power consumption of the CCFL backlights and the LED backlight are 22.3 Watt and 16.57 Watt, respectively. In Figure 7-4(a), the image of the CCFL backlight and the LED backlight are the same. In Figure 7-4 (b), the two images still resemble to each other. But in Figure 7-4(c), the pixels are saturated.

7.2.1 Power Savings

We applied our algorithm when various benchmark images were displayed on our platform. The benchmark images and power measurement results are shown in Table 7-1 and Table 7-2. The full power consumption of the LED backlights is 23.06 Watt. When the color difference constraint of $\Delta E_{ab}^* \leq 1$ and $\Delta E_{ab}^* \leq 2$ were given respectively, the LED backlight power savings of range from 19% to 48% at the color difference constraint $\Delta E_{ab}^* \leq 1$ and 30% to 55% at the color difference constraint $\Delta E_{ab}^* \leq 2$.

Table 7-1. Benchmark images.

			
Image1	Image2	Image3	Image4
			
Image5	Image6	Image7	Image8
			
Image9	Image10	Image11	Image12

Table 7-2. Optimal solutions for benchmark images subject to $\Delta E_{ab}^* \leq 1$ and $\Delta E_{ab}^* \leq 2$.

Image	R-Power (W)		G-Power (W)		B-Power (W)		Power Saving (%)	
	$\Delta E_{ab}^* \leq 1$	$\Delta E_{ab}^* \leq 2$	$\Delta E_{ab}^* \leq 1$	$\Delta E_{ab}^* \leq 2$	$\Delta E_{ab}^* \leq 1$	$\Delta E_{ab}^* \leq 2$		
1	4.92	3.72	6.93	5.99	5.51	5.32	24.72	34.84
2	3.84	3.36	7.25	5.99	5.32	4.18	28.86	41.35
3	4.68	5.64	8.82	6.62	5.32	2.28	35.32	36.97
4	2.64	4.32	7.25	7.25	1.9	4.56	23.55	30.07
5	5.28	5.4	5.99	6.3	5.32	4.18	19.97	31.14
6	5.52	5.52	7.25	6.62	2.47	2.09	33.93	38.31
7	4.56	4.92	7.56	5.99	5.51	4.94	28.08	31.29
8	4.32	2.4	7.25	6.93	5.51	0.95	48.89	55.42
9	5.28	3.96	7.25	6.93	4.56	5.13	25.95	30.53
10	5.04	4.92	8.82	6.62	6.08	4.56	25.91	30.2
11	4.2	3.48	5.99	5.04	2.28	1.71	45.95	55.44
12	5.64	4.56	6.62	6.93	2.66	4.37	21.78	31.22

7.2.2 Performance

Figure 7-5 shows the performance of the original images and backlight scaling images while giving the constraint of $\Delta E_{ab}^* \leq 2$. The power savings of these images can be found in Table 7-2. The image quality can be preserved with our backlight scaling algorithm. Simultaneously, the purpose of reducing the power consumption of the LED backlights can be

achieved.

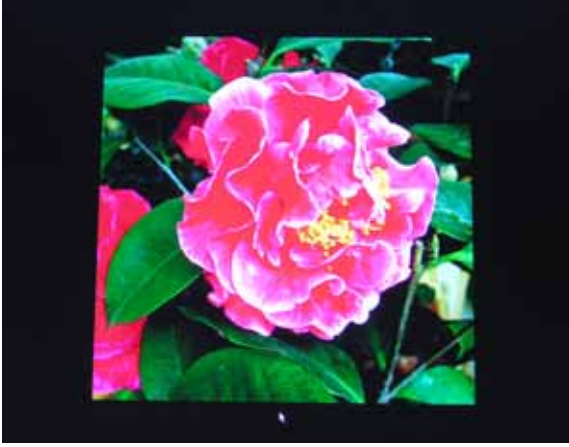
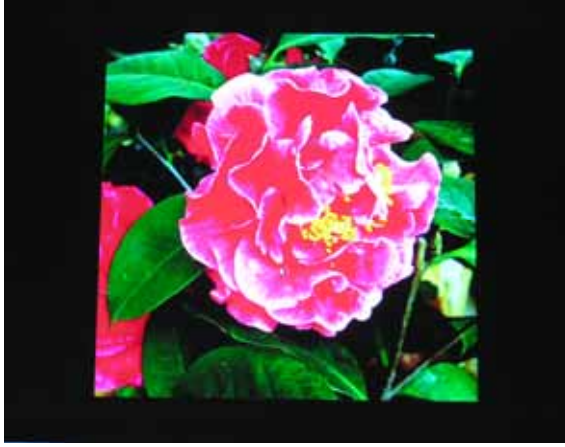
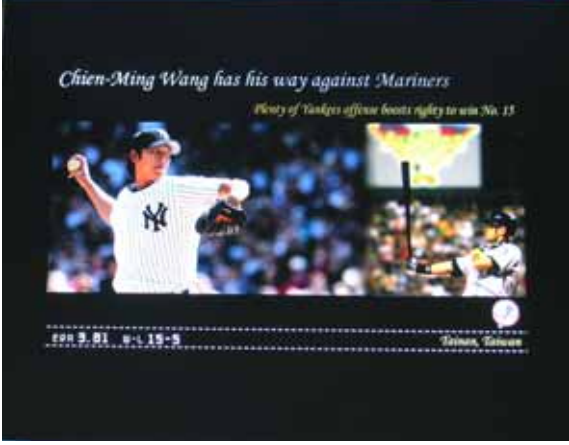
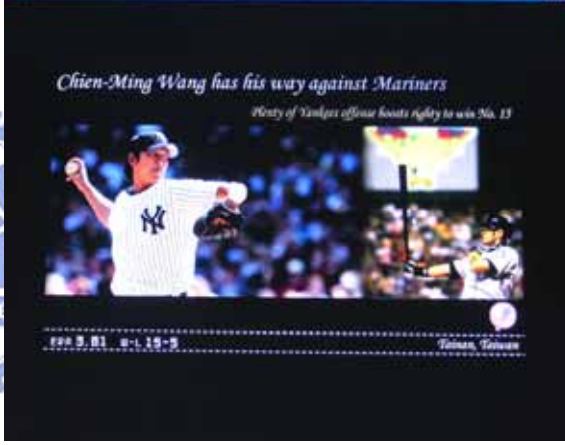


Original images	Scaling images
	
	
	

Figure 7-5. Comparison between the original images and the scaling images.

7.2.3 Viewing Angle Enhancement for Visual Effect

For TN mode LCDs, the refraction ratio of liquid crystals depends on the applied voltage and wavelength, which usually have serious color shift in the vertical viewing angle. The LCD color shift degrades the image quality and detains purchase decision of consumers, caused by the phase retardation variance of the liquid crystals. The LCD color shift is dependent on a number of variables including transmittance, chroma, and viewing angle. Figure 7-6 shows the color shift of VX912 at different viewing angles. From Figure 7-6(a), (b), and (c) we observe that the luminance reduces from the normal angle to the outside angle. It is the most obvious in the vertical angle. The luminance variations will cause the contrast degradation.

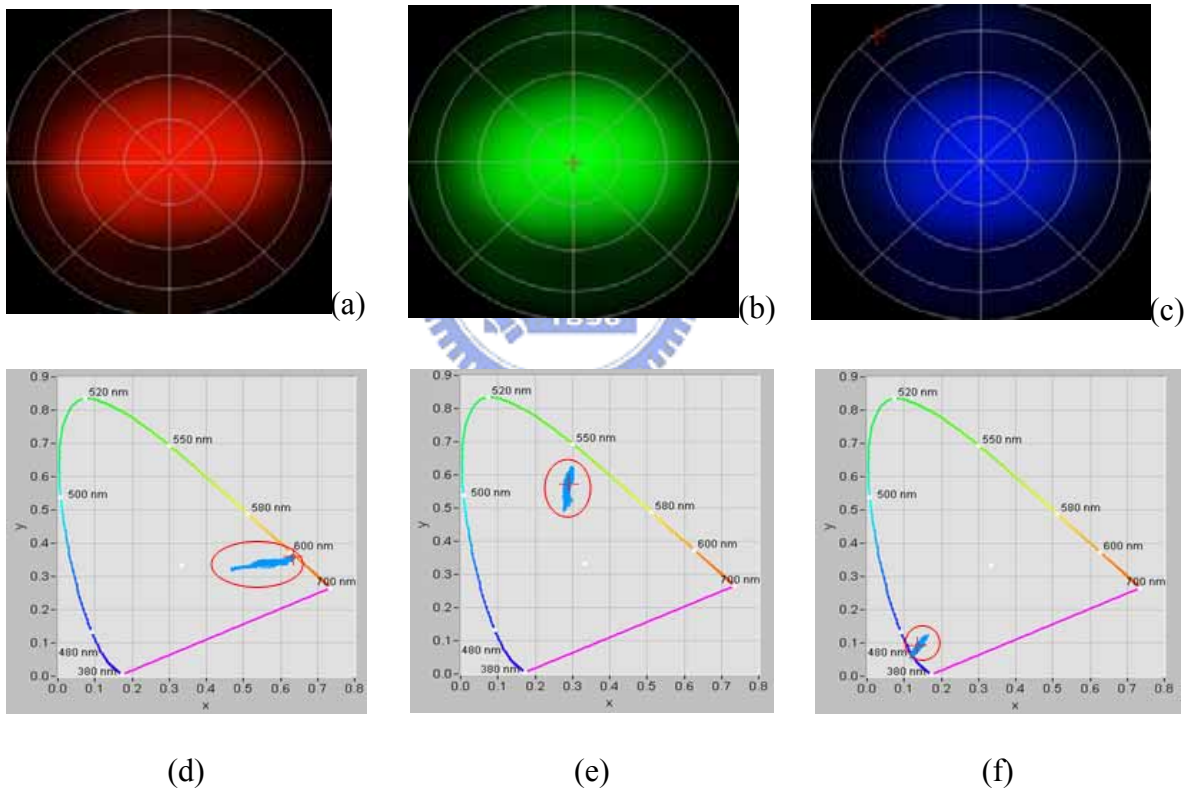


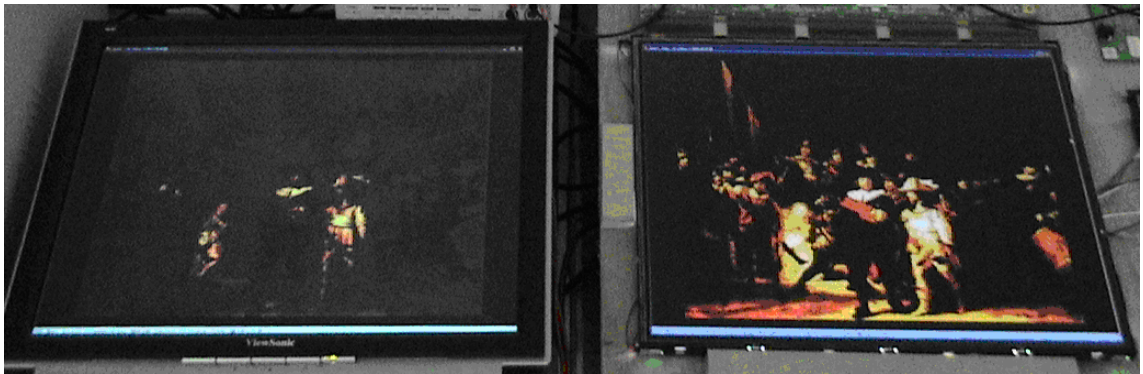
Figure 7-6. Color shift of the panel of VX912 at different viewing angles.

Base on our backlight scaling algorithm, the image contrast can be enhanced while the viewing angle is not normal. The contrast degradation of the image on the TN mode LCDs can be improved. We can get better visual effect at different viewing angles. Figure 7-6 shows

the image without using backlight scaling algorithm and with backlight scaling algorithm while we tilted the two panels vertically. We can perceive the better image contrast of the right-side panel in Figure 7-7(b).



(a) Image without using backlight scaling algorithm



(b) Image with using backlight scaling algorithm

Figure 7-7. The panels were tilted about 30° vertical viewing angle.

7.3 Summary

We have implemented the backlight scaling algorithm for minimizing power consumption of RGB LED-backlight TFT-LCDs. The proposed algorithm was implemented by an FPGA board. The image quality can be preserved as the backlight intensity is dimmed. For the benchmark images, up to 55% of power consumption can be reduced when the color difference constraint of $\Delta E_{ab}^* \leq 2$ was given. Moreover, the backlight scaling algorithm enhances the image contrast of TN-mode LCD at different viewing angles.

Chapter 8

Conclusion and Future Direction

8.1 Conclusion

Today, TFT-LCD is the most common display in the mobile electronic devices. It is also one of the components which contribute the most power consumption in the mobile electronics. The TFT-LCD backlight dominates the power consumption of the whole system. For prolonging the battery lifetime of the mobile electronic devices, the power consumption have to be reduced.

Our goal is to reduce the power consumption of TFT-LCD backlight. The technique of backlight scaling is used to achieve the purpose. The technique of backlight scaling decreases the backlight intensity to conserve power consumption while preserving the visual quality. The technique need to employ algorithm for implementing the backlight dimming and image processing. We proposed the Chromaticity and Luminance Scaling algorithm based on visual perception for minimizing power consumption of LED backlight TFT-LCDs. The CLS algorithm consists of two phases. The chromaticity scaling is guided by the CIELAB color difference to scale the red, green and blue backlight individually. The luminance scaling is based on the prior Concurrent Brightness and Contrast Scaling algorithm, which was solidified by a series psychophysical vision experiments. We also conducted a psychophysical experiment, in which the interaction between perceived brightness and contrast was validated. Another psychophysical experiment gave luminance algorithm a strong persuasion to adopt the CBCS algorithm.

Finally, we prototyped an experimental LED backlight platform for characterizing its power consumption in red, green, and blue. The proposed algorithm was implemented by an

FPGA board. For the benchmark images, up to 55% of power consumption can be reduced. At the same time, reducing the power consumption of LED backlights can prolong the LED lifetime and reduce the LED color shift due to thermal effects. Moreover, the light leakage of TFT-LCD results in angular-dependent luminance reduction and color shift. The backlight scaling algorithm increasing panel transmittance can avoid the light leakage of normally-white TFT-LCDs. This process can reduce the angular-dependent color shift of TFT-LCDs. In addition, our algorithm can increase the dynamic contrast ratio, and the image quality can be preserve.

8.2 Future Direction

The core in the technique of backlight scaling is the algorithm. Although the interaction between perceived brightness and contrast has been validated, the psychophysical experiments will be continued. The psychophysical experiments require to be improved, and then the consideration of Bartleson-Breneman effect also will be included. The model of perceived image brightness and contrast will be created by the psychophysical experiments. The psychophysical experimental results will be utilized to refine our algorithm. However, the surrounding-aware LCD is not commercially available yet. For implementation, the ambient light can be quantified by installing a photo sensor. Moreover, the experimental platform will be transfer to small-sized panels. The final goal is develop an Application Specific Integrated Circuit (ASIC) to replace the FPGA board. It can be fabricated as an adapter between a laptop computer and a TFT-LCD or built into the internal circuit of a TFT-LCD.

References

- [1] A. Mahesri and V. Vardhan, "Power Consumption Breakdown on a Modern Laptop," Workshop on Power Aware Computing Systems, 37th International Symposium.
- [2] K. Meinstein et al., "A Low-Power High-Voltage Column/Dot Inversion Drive System," *Society for Information Display 1995 Digest*, pp.391-394.
- [3] B-D. Choi and O-K. Kwon, "Stepwise data driving method and circuits for low-power TFT-LCDs," *IEEE Transaction on Consumer Electronics*, vol. 46, Nov. 2000, pp. 1155-1160.
- [4] B-D. Choi and O-K Kwon, "A Low-Power data driver with stepwise driving method for TFT-LCDs," *Society for Information Display 2001 Digest*, pp. 273-275.
- [5] A. Erhart and D. McCartney, "Charge conservation implementation in a ultra low power AMLCD column driver utilizing pixel inversion," *Society for Information Display 1997 Digest*, pp. 23-26.
- [6] I. Hwang et al., "Image Synchronized Brightness Control," *Society for Information Display 2001 Digest*, pp. 492-493.
- [7] I. Choi, H. Shim, and N. Chang, "Low-Power color TFT-LCD display for hand-held embedded systems," *Proc. Int. Symp. Low-Power Electronics and Design*, Aug. 2002, pp. 112-117.
- [8] F. Gatti, A. Acquaviva, L. Benini, and B. Ricco, "Low power control techniques for TFT LCD displays," in *Proc. Int. Conf. Compilers, Architecture, and Synthesis for Embedded Systems*, Oct. 2002, pp. 218-224.
- [9] N. Chang, I. Choi and H. Shim, "DLS: Dynamic Backlight Luminance Scaling of Liquid Crystal Display," *IEEE Transaction on Very Large Scale Integration Systems*, Vol.12, No. 8, Aug. 2004, pp. 837-846.
- [10] W-C. Cheng and M. Pedram, "Power Minimization in a Backlit TFT-LCD by Concurrent

- Brightness and Contrast Scaling,” *IEEE Transactions on Consumer Electronics*, Vol. 50, No. 1, Feb. 2004, pp. 25-32.
- [11] W-C. Cheng, “Power-minimization of LED backlight in a color sequential display,” *Society for Information Display 2005 Digest*, pp. 1384-1387.
- [12] A. Iranli, H. Fatemi, M. Pedram, “HEBS: Histogram equalization for backlight scaling,” *Proc. of Design Automation and Test in Europe*, March 2005, pp. 346-351.
- [13] N. Raman, G. J. Hekstra, “Content based contrast enhancement for liquid crystal displays with backlight modulation,” *IEEE Transactions on Consumer Electronics*, Vol. 50, No. 1, Feb. 2005, pp. 18-21.
- [14] S. Pasricha, S. Mohapatra, M. Luthra, N. Dutt, and N. Venkatasubramanian, “Reducing backlight power consumption for streaming video applications on mobile handheld devices,” *ESTIMedia*, 2003.
- [15] S. Pasricha et al., “Dynamic Backlight adaptation for low power handheld devices,” *IEEE Design and Test (IEEE D&T)*, Sep. 2004, pp. 398-405.
- [16] L. Cheng et al., “Quality adapted backlight scaling (QABS) for video streaming to mobile handheld devices,” *LNCS*, Apr. 2005, pp. 662-671.
- [17] R. Cornea et al. “Software Annotations for Power Optimization on Mobile Devices,” *Proc. of Design Automation and Test in Europe*, May 2006, pp. 684-689.
- [18] A. Iranli, M. Pedram, “DTM: Dynamic tone mapping for backlight scaling,” *Proc. of Design Automation Conference*, June 2005, pp. 612-517.
- [19] L. Zhong and N. K. Jha, “Energy efficiency of handheld computer interfaces: limits, characterization and practice,” *MobiSis 2005*, June 2005, pp. 247-260.
- [20] G. Wyszecki and W. S. Stiles, *Color Science*, John Wiley and Sons, 1982.
- [21] R. W. G. Hunt, *Measuring Colour, 3rd Ed.*, Foutain Press, 1998.
- [22] M. D. Fairchild, *Color Appearance Models, 2nd Ed.*, Wiley-IS&T, Chichester, 2005.
- [23] R. Blake, R. Sekuler, *Perception, 5th Ed.*, McGraw-Hill, NY, 2006.

- [24] J. C. Stevens and S. S. Stevens, "Brightness functions: effects and adaptation," *J. Opt. Soc. Am.*, 1963, Vol. 53, pp. 375-385.
- [25] M. D. Fairchild, "Considering the Surround in Device Independent color Imaging," *Color Research and Application*, pp. 352-363(1995).
- [26] C. J. Bartleson and E. J. Breneman, "Brightness perception in complex fields," *J. Opt. Soc. Am.*, 1967, Vol. 57, pp. 953-957.
- [27] C-M. Liu and M. D. Fairchild, "Measuring the relationship between perceived image contrast and surround illumination," *IS&T/SID Twelfth color imaging conference*, 2004, pp. 282-288.
- [28] E. J. Breneman, "Perceived saturation in complex stimuli viewed in light and dark surrounds," *J. Opt. Soc. Am.*, 1977, Vol. 67, pp. 657-662.
- [29] C. J. Bartleson, "Optimum Image Tone Reproduction," *J. SMPTE*, **84**, 613-618, 1975.
- [30] AUO Corp., *M190EN04 V.2 Liquid Crystal Display*.
- [31] Xilinx, *Spartan-3 Starter Kit Board User Guide*.
- [32] National Semiconductor, *DS90C387A/DS90CF388A, Dual Pixel LVDS Display Interface/FPD-Link*, 2006.